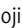




ARTICLE

Eps15/Pan1p is a master regulator of the late stages of the endocytic pathway

Mariko Enshoji^{1*}, Yoshiko Miyano^{1*}, Nao Yoshida^{1*}, Makoto Nagano¹, Minami Watanabe¹, Mayumi Kunihiro¹, Daria E. Siekhaus², Junko Y. Toshima^{1,3}, and Jiro Toshima¹

Endocytosis is a multistep process involving the sequential recruitment and action of numerous proteins. This process can be divided into two phases: an early phase, in which sites of endocytosis are formed, and a late phase in which clathrin-coated vesicles are formed and internalized into the cytosol, but how these phases link to each other remains unclear. In this study, we demonstrate that anchoring the yeast Eps15-like protein Pan1p to the peroxisome triggers most of the events occurring during the late phase at the peroxisome. At this ectopic location, Pan1p recruits most proteins that function in the late phases—including actin nucleation promoting factors—and then initiates actin polymerization. Pan1p also recruited Prk1 kinase and actin depolymerizing factors, thereby triggering disassembly immediately after actin assembly and inducing dissociation of endocytic proteins from the peroxisome. These observations suggest that Pan1p is a key regulator for initiating, processing, and completing the late phase of endocytosis.

Introduction

Clathrin-mediated endocytosis (CME) is a fundamental cellular function involved in various physiological processes, such as nutrient uptake, receptor internalization, synaptic vesicle recycling, and defense against pathogens. The molecular mechanism regulating CME is highly conserved in eukaryote cells, and it can be roughly divided into an early phase and a late phase. The early-phase proteins, including early coat proteins, function in determining the endocytic-site location and recruiting cargo, whereas the late-phase proteins, including mid/late coat proteins, actin and actin regulators, and amphiphysin, induce deeply invaginated membranes by triggering transient actin assembly and facilitating scission (Kaksonen and Roux, 2018). The molecular mechanisms underlying each phase have been investigated intensively, but how these phases link to each other remains unclear. Thus, clarifying the molecular mechanism regulating transitions between the phases is important for understanding how the progression of endocytosis is regulated. In previous studies, it has been shown that endocytic vesicle formation in the late phase can still occur even when genes encoding several early-phase proteins are simultaneously deleted, suggesting there is a degree of autonomy in the execution of the late phase in endocytosis (Brach et al., 2014).

One promising candidate protein for coupling the late endocytic phase to early phase is the yeast Eps15-like protein

Pan1p, which serves as a key scaffolding protein in the late stages of the yeast CME pathway. Previous studies have demonstrated that Pan1p interacts with numerous endocytic proteins, including clathrin adaptors and coat proteins (Tang et al., 2000; Wendland and Emr, 1998; Wendland et al., 1999), and that these interactions are negatively regulated by the Prk1 family protein kinases, Prk1p and Ark1p (mammalian GAK/AAK1 homologs; Smythe and Ayscough, 2003). These kinases are recruited to endocytic sites just after the initiation of actin assembly, and they phosphorylate several endocytic proteins, including Pan1p, to disassemble the CCV (Cope et al., 1999; Toret et al., 2008; Zeng et al., 2001). The EH domain protein End3p and Pan1p form a stable complex, which is not regulated by Ark1p/Prk1p phosphorylation (Sun et al., 2015b; Toshima et al., 2007), and the complex, together with Sla1p, seems to function as a core scaffold that resembles mammalian intersectins (Goode et al., 2015; Yamada et al., 1998). Recent studies using the auxin-inducible degron system for rapid deletion of Pan1p alone or Pan1p and End3p simultaneously from the cell have suggested that endocytic site initiation and actin assembly are separable processes linked by a Pan1p complex (Bradford et al., 2015; Sun et al., 2015a). These observations clearly indicate the importance of Pan1p in the late stages of endocytosis, although the mechanisms

¹Department of Biological Science and Technology, Tokyo University of Science, Katsushika-ku, Tokyo, Japan; ²Institute of Science and Technology Austria, Klosterneuburg, Austria; ³School of Health Science, Tokyo University of Technology, Ota-ku, Tokyo, Japan.

*M. Enshoji, Y. Miyano, and N. Yoshida contributed equally to this paper. Correspondence to Jiro Toshima: jtosiscb@rs.tus.ac.jp; Junko Y. Toshima: toshimajk@stf.teu.ac.jp.

© 2022 Enshoji et al. This article is distributed under the terms of an Attribution-Noncommercial-Share Alike-No Mirror Sites license for the first six months after the publication date (see <http://www.rupress.org/terms/>). After six months it is available under a Creative Commons License (Attribution-Noncommercial-Share Alike 4.0 International license, as described at <https://creativecommons.org/licenses/by-nc-sa/4.0/>).

whereby Pan1p drives the progression of endocytosis from the early to late stage remain unknown.

In addition to its role as a scaffolding protein, Pan1p functions as an actin regulator during CCV internalization. Previous studies have revealed that the actin cytoskeleton plays a critical role in the formation and internalization of CCVs and the subsequent transport of endocytic vesicles to the early endosome (Goode et al., 2015; Kaksonen and Roux, 2018; Weinberg and Drubin, 2012). In yeast endocytosis, several actin nucleation promoting factors (NPFs), such as the yeast WASP homolog Las17p (Winter et al., 1999), the type I myosins Myo3p and Myo5p (Evangelista et al., 2000), the actin-binding protein Abp1p (Goode et al., 2001), and Pan1p (Duncan et al., 2001), promote actin polymerization to generate the force required for CCV formation and internalization. Among these NPFs, Las17p and Myo3p/5p, which form a complex with yeast WIP (Vrp1p), have been shown to have high activity and play an important role in the initiation of actin assembly at sites of endocytosis (Sun et al., 2006). In contrast, Pan1p has a lower NPF activity compared to Las17p and Myo3p/5p, and mutation in the Arp2/3 complex binding region of Pan1p causes only a minor defect in actin polymerization at the endocytic sites (Sun et al., 2006; Toshima et al., 2005). However, the dephosphorylation-mimicking mutant of Pan1p binds to F-actin with high affinity, and its expression causes aberrant actin polymerization (Toshima et al., 2005; Toshima et al., 2016). Interestingly, this Pan1 mutant also leads to stable interaction between endocytic vesicles and actin cables (Toshima et al., 2016). Thus, although Pan1p seems to play somewhat important roles in actin-mediated vesicle internalization and transport, details of its contribution to actin assembly during endocytosis remain ambiguous.

In the present study, we sought to clarify the function of Pan1p during the progression of the late steps of endocytosis using cells in which Pan1p had been relocated to the peroxisome using a rapamycin-induced dimer formation system. We found that anchoring Pan1p to the peroxisome triggered most of the events occurring during the late stage of endocytosis, including recruitment of the mid- and late-coat proteins and adaptors, initiation of actin polymerization, and disassembly of the endocytic machinery. Pan1p anchored to the peroxisome also recruited actin cables to the peroxisome simultaneously with the initiation of actin polymerization. These findings suggest that the recruitment of Pan1p to endocytic sites is sufficient to initiate and complete the later processes of clathrin-mediated endocytosis.

Results

Localization of Pan1p to the peroxisome triggers *in situ* actin polymerization

In comparison to Las17p and Myo3p/5p, Pan1p has lower NPF activity, and mutation in the Arp2/3 complex binding region of Pan1p causes only a minor defect of actin polymerization at endocytic sites (Sun et al., 2006; Toshima et al., 2005). Thus, it has been unclear whether Pan1p is required for the initiation of actin polymerization at endocytic sites. To investigate this issue, we ectopically anchored Pan1p to peroxisomes using the FRB and

FKBP domains, which form stable dimers in the presence of rapamycin (Banaszynski et al., 2005). We first employed Pex-FRB-mCherry, a fusion protein containing the peroxisomal membrane-targeting signal of Pex3p coupled to mCherry fluorescent protein and FRB (Fig. 1 A) and confirmed that it became localized at Pex3-GFP-labeled peroxisomes (Fig. S1 A). We also fused Pan1p to GFP and FKBP (Pan1-GFP-FKBP; Fig. 1 A) and tested whether the anchoring of Pex-FRB-mCherry to peroxisomes upon the addition of rapamycin resulted in the recruitment of Pan1p to peroxisomes. Before rapamycin addition, little colocalization between Pan1-GFP-FKBP and Pex-FRB-mCherry was observed, but after rapamycin addition, ~94 and ~98% colocalization was observed at 15 and 30 min, respectively (Fig. 1, B and C). To assess actin polymerization, we examined the localization of a marker for this process, Abp1-GFP, in a strain expressing Pex-FRB-mCherry and Pan1-FKBP (Fig. 1 D). When Pan1-FKBP was anchored to peroxisomes, around ~62.0% of Abp1-GFP was locally recruited, but the recruitment was remarkably inhibited in the presence of the actin-sequestering drug, Latrunculin A (LatA), suggesting that Abp1p localization at peroxisomes requires F-actin (Fig. 1, E and F). To directly confirm that actin polymerization occurs at the peroxisome, we used GFP-fused actin (GFP-Act1) instead of Abp1-GFP and investigated whether GFP-Act1 was recruited to peroxisomes upon treatment with rapamycin. Similar to Abp1-GFP, localization of GFP-Act1 at the peroxisomes was clearly observed (Fig. 1, G and H). To exclude the possibility that the localization of Pan1p and actin to the peroxisome are caused by the tethering of endocytic vesicles to the peroxisome, we examined the localization of the fluorescent endocytic tracer FM4-64 in the presence of rapamycin. When added to wild-type cells, FM4-64 is immediately incorporated into the plasma membrane and internalized via bulk-phase endocytosis. FM4-64 is then transported to the endosomes at 5–10 min, but FM4-64-labeled puncta were rarely localized at peroxisomes, although Abp1-mCherry is efficiently recruited there (Fig. S1, B and C). LatA treatment caused a decrease of Abp1p recruitment to the peroxisome to ~4.4% at 20 min after treatment, but the recruitment recovered to ~69.5% at 20 min after washing away LatA (Fig. 1, E and F; and Video 1). These observations suggest that Pan1p has the ability to initiate actin polymerization *in vivo* by itself or through its interacting proteins.

Pan1p induces actin polymerization in a coordinated manner by recruiting other NPFs

We next utilized the Arp2/3 complex inhibitor CK-666 that specifically disassembles actin assembly at the endocytic sites in yeast (Nolen et al., 2009). The effect of CK666 was fully reversible, and Abp1p disappeared from peroxisomes rapidly 1 min after the treatment but the localization recovered within 2 min after washing away the drug (Fig. 2, A and B; and Video 2). To examine the dynamics of actin polymerization at the peroxisome upon Pan1p anchoring, we expressed GFP-fused Pan1-FKBP and CFP-fused Abp1p in a strain expressing Pex-FRB-mCherry (Fig. 2 C). Triple-color live cell analysis showed that Pan1p and Abp1p behaved differently at the peroxisome in cells treated with rapamycin. Pan1p persisted at the peroxisome

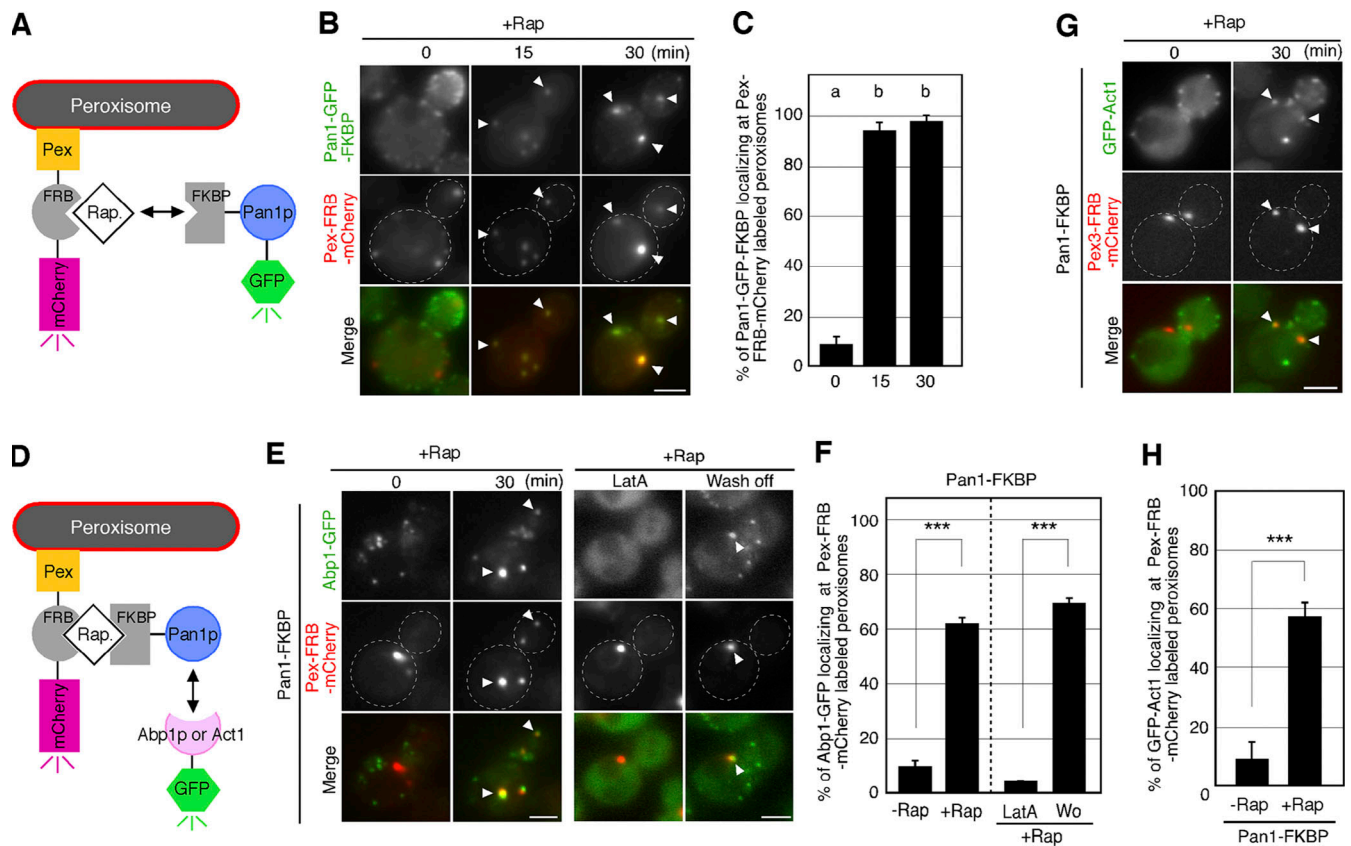


Figure 1. Ectopically localized Pan1p leads to actin polymerization at the peroxisome. (A and D) Schematic diagrams of the inducible peroxisome redistribution assay. **(B)** Each image pair was acquired at 0, 15, and 30 min after rapamycin addition. White arrowheads indicate examples of co-localization. **(C)** Quantification of the percentage of Pan1-GFP-FKBP localizing at Pex-FRB-mCherry-labeled peroxisomes. Data show the mean \pm SD from three experiments ($n = 50$ puncta for each experiment). **(E)** Localization of Abp1-GFP and Pex-FRB-mCherry at 0 or 30 min after rapamycin addition. Right image pairs in E were acquired at 20 min after 200 μ M LatA treatment, and at 19 min after washing away LatA. **(F)** Quantification of the percentage of Abp1-GFP co-localizing with Pex-FRB-mCherry in the indicated conditions. Data show the mean \pm SD from three experiments ($n > 30$ puncta for each experiment). ***, P value < 0.001 , unpaired t test with Welch's correction. **(G)** Localization of GFP-Act1 and Pex-FRB-mCherry at 0 or 30 min after rapamycin addition. Cells were grown to log phase at 25°C and each image pair was acquired before or after rapamycin addition. **(H)** Quantification of the percentage of GFP-Act1 co-localizing with Pex-FRB-mCherry in the indicated conditions upon the expression of Pan1-FKBP. Data show the mean \pm SD from three experiments ($n = 50$ puncta for each experiment). ***, P value < 0.001 , unpaired t test with Welch's correction. Scale bars, 2.5 μ m.

labeled by Pex-FRB-mCherry, whereas Abp1p regularly appeared at the peroxisome and then disappeared (Fig. 2, D and E; and Video 3). Quantification of the fluorescence intensities of these proteins confirmed that Pan1p remained localized to the peroxisome constantly and revealed that Abp1p showed dynamic localization that increased gradually and then decreased after reaching a maximum (Fig. 2 F). We noticed that the behavior of Abp1p at the peroxisome was similar to that at endocytic sites (Kaksonen et al., 2003).

We sought to assess if Pan1p recruits interacting proteins to modulate actin assembly. At the endocytic site, actin polymerization is regulated by several actin nucleation promoting factors (NPFs), including Myo3/5p, Las17p, Abp1p, and Pan1p (Goode et al., 2015; Weinberg and Drubin, 2012). As it has been reported that Las17p and Myo3p/5p have higher NPF activity relative to Pan1p and Abp1p and that their NPF activities are most important for endocytic vesicle formation, we next examined if these proteins are recruited to the peroxisome, dependent on Pan1p (Fig. 2 G). Before the addition of rapamycin,

Las17p and Myo3/5p were rarely localized at the peroxisome (Fig. 2 I and Fig. S1 D), but after Pan1-FKBP had become anchored to the peroxisome upon treatment with rapamycin, around $\sim 49.3\%$, $\sim 19.3\%$, and $\sim 42.0\%$ of Las17p, Myo3p, and Myo5p were recruited to the peroxisome, respectively (Fig. 2, H and I). We also examined whether Las17-, Myo3-, or Myo5-FKBP was conversely capable of recruiting Pan1p to the peroxisome; however none of these proteins could (Fig. 3, A and B). Surprisingly, direct anchoring of Las17-, Myo3-, or Myo5-FKBP to the peroxisome did not induce actin polymerization, as assessed by Abp1p recruitment (Fig. 3, C-E and Fig. S1 E). A previous study has shown that accumulation of Las17p and Myo3p above a certain threshold at endocytic sites triggers actin polymerization (Sun et al., 2017). Thus, we next examined if increasing amounts of the NPFs can induce actin polymerization at the peroxisome. Consistent with the previous model, simultaneous anchoring of Las17p, Myo3p, and Myo5p, or Myo3p and Myo5p alone, could substantially cause actin polymerization, as assessed by Abp1p recruitment ($\sim 44.7\%$ and $\sim 26.7\%$, respectively; Fig. 4, A and B; and

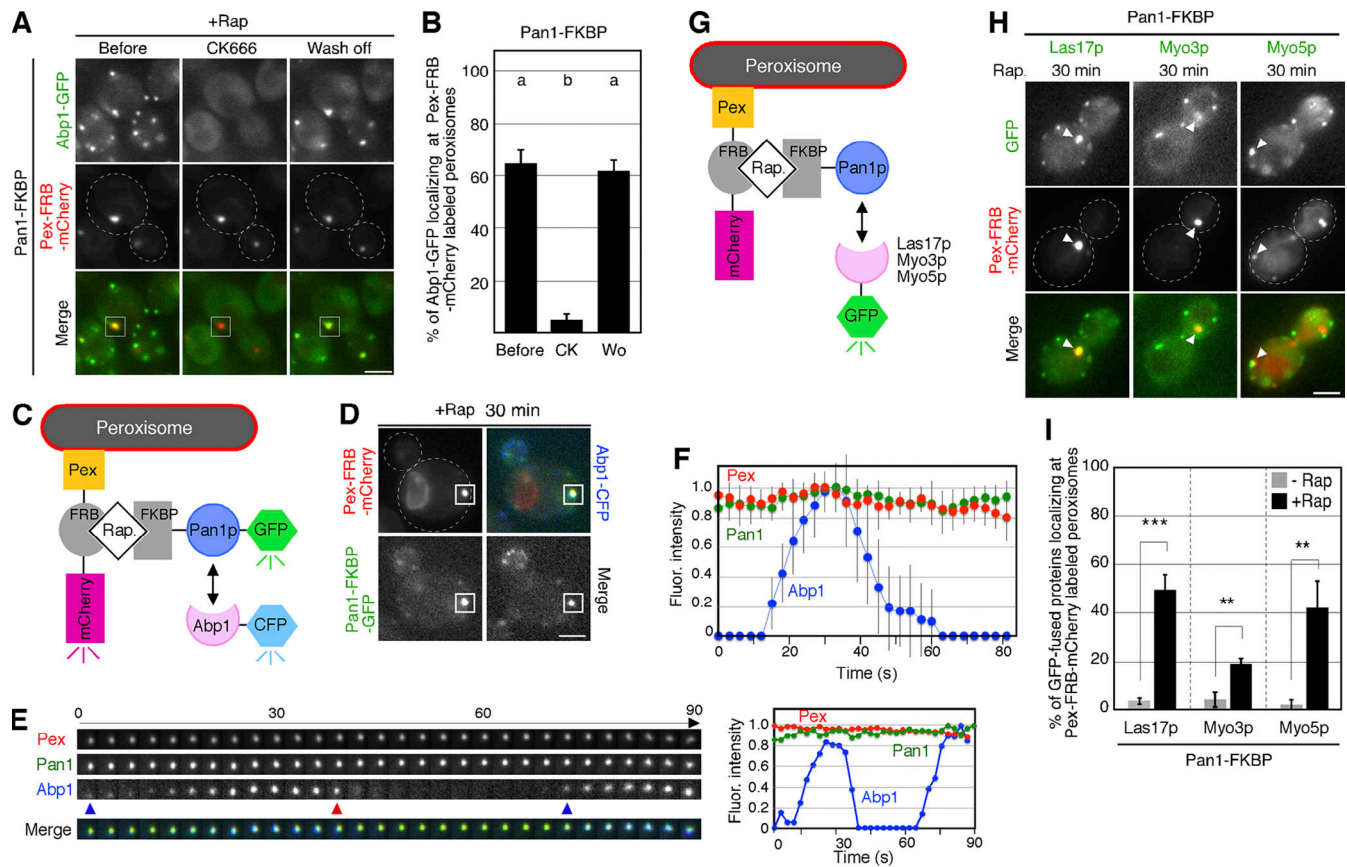


Figure 2. Pan1p recruits other NPFs and triggers actin polymerization. (A) Localization of Abp1-GFP and Pex-FRB-mCherry before or at 1 min 45 s after CK666 treatment in the presence of rapamycin (left and center image pairs). Right image pair in A was acquired at 1 min 35 s after washing away CK666. (B) Data show the mean \pm SD from three experiments ($n = 50$ puncta for each experiment). Different letters indicate significant difference between indicated times at $P < 0.001$, one-way ANOVA with Turkey's post-hoc test. (C) Schematic diagrams of the inducible peroxisome redistribution assay. Pan1-GFP-FKBP was co-expressed with Pex-FRB-mCherry in cells expressing Abp1-CFP. (D) Localization of Pan1-GFP-FKBP, Pex-FRB-mCherry, and Abp1-CFP at 30 min after rapamycin addition. (E) The time series of each protein in the boxed area (D) are shown in the lower panels. Blue or red arrowheads indicate the timing of the appearance or disappearance respectively of Abp1-CFP signal. Quantification of fluorescence intensities for each protein in the boxed area is shown in the right panel. (F) Averaged fluorescence intensities as a function of time for each protein ($n = 10$ independent peroxisomes). (G) FKBP-tagged Pan1p was co-expressed with Pex-FRB-mCherry in cell expressing indicated GFP-tagged proteins. (H) Each image pair was acquired at 30 min after rapamycin addition. White arrowheads indicate examples of co-localization. (I) Quantification of the percentage of each GFP-tagged protein localizing at Pex-FRB-mCherry-labeled peroxisomes. Data show the mean \pm SD from three experiments ($n = 50$ puncta for each experiment). ***, P value < 0.001 , **, P value < 0.01 , unpaired t test with Welch's correction. Scale bars, 2.5 μ m.

Fig. S1 F). Intriguingly, Abp1p regularly appeared and disappeared when Pan1p was anchored (Fig. 2 E), whereas when Las17p and/or Myo3p/5p were anchored, Abp1p was stably localized at peroxisome (Fig. 4, C and D). Anchoring of overexpressed Las17p also induced similar actin polymerization (Fig. 4, E–H). To further clarify the contribution of these NPF activities for actin polymerization at the peroxisome, we utilized inactive or deletion mutants. When a Pan1 mutant that lacks both actin binding and Arp2/3 binding regions (Pan1 Δ WA) is anchored to the peroxisome, actin polymerization occurred at similar levels to that seen upon the anchoring of wild-type Pan1p (Fig. 4, I and J). This suggests that Pan1p's NPF activity is not essential for the initiation of actin polymerization. In contrast, the presence of the *las17* Δ WCA mutant, which lacks the C-terminal Arp2/3 complex activation region, reduced the frequency of actin polymerization at the peroxisome (Fig. 4, I and J), suggesting that Las17p's NPF activity contributes to the initiation of actin

polymerization. Deletion of either Myo3p or Myo5p did not affect actin polymerization at the peroxisome (Fig. 4 J and Fig. S1 G), probably because of the redundant function of these proteins (Anderson et al., 1998). Thus, FKBP-tagged Pan1p was able to recruit all other NPFs to the peroxisome when anchored there, and among them Las17p and Myo3p/5p seemed to be most important for actin polymerization at the peroxisome.

Pan1p regulates mid- and late-coat protein assembly

The timing of the appearance and disappearance of many endocytic proteins at endocytic sites has been clarified, and these proteins can be categorized into at least five modules: early proteins, early/mid/late coat, WASp/myosin, actin, and scission modules (Lu et al., 2016). We sought to determine which endocytic proteins are recruited to the peroxisome dependent on Pan1p. To this end, we employed Syp1p and Edelp as markers of early proteins, Yap1801p as a marker of early coat protein, Sla2p,

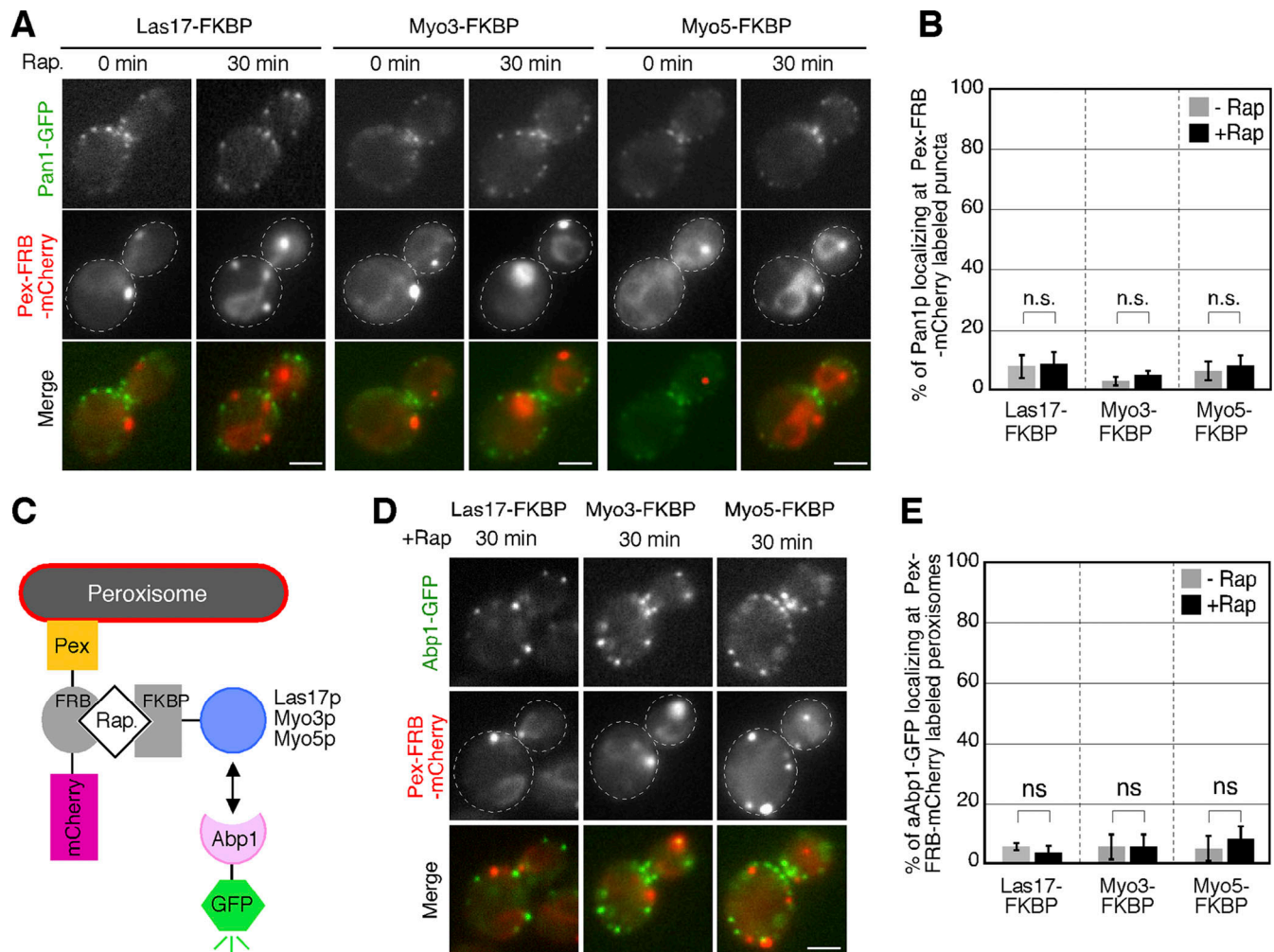


Figure 3. Direct anchoring of Las17-, Myo3-, or Myo5-FKBP to the peroxisome does not recruit Pan1p to the peroxisome. (A) Cells expressing Pan1-GFP, Pex-FRB-mCherry, and FKBP-tagged Las17p (left panels), Myo3p (center panels), or Myo5p (right panels) were grown to log phase at 25°C, and each image pair was acquired before or 30 min after rapamycin addition. (B) The percentage of Pan1-GFP co-localizing with Pex-FRB-mCherry-labeled peroxisomes in the presence of the indicated other FKBP-fusion protein before and after rapamycin addition. Data show the mean \pm SD from at least three experiments ($n > 30$ puncta for each experiment). (C) FKBP-tagged Las17p, Myo3p, or Myo5p was co-expressed with Pex-FRB-mCherry and Abp1-GFP. (D) Each image pair was acquired at 30 min after rapamycin addition. (E) Quantification of the percentage of each GFP-tagged protein localizing at Pex-FRB-mCherry-labeled peroxisomes. Data show the mean \pm SD from three experiments ($n = 50$ puncta for each experiment). ns, non-statistically significant, unpaired *t* test with Welch's correction. Scale bars, 2.5 μ m.

Ent1p, and Ent2p as markers of mid-coat proteins, and End3p and Sla1p as markers of late-coat proteins (Fig. 5 A; Weinberg and Drubin, 2012). We fused GFP to these proteins and expressed them in a strain expressing Pex-FRB-mCherry and Pan1-FKBP (Fig. 5 B). None of these proteins localized at the mCherry-labeled peroxisome before the addition of rapamycin (Fig. 5 E and Fig. S2 A). At 30 min after rapamycin addition, however, the mid- and late-coat proteins, End3p, Sla2p, Ent1p, and Ent2p, changed their localization to mCherry-labeled peroxisomes, whereas the localization of the early proteins, Sy1p and Ede1p, and the early coat protein, Yap1801p, was not affected (Fig. 5 C). The recruitment of mid- and late-coat proteins by Pan1-FKBP was not affected in the presence of LatA (Fig. 5 D), indicating that these interactions are not mediated by actin filaments. Among the proteins recruited to mCherry-labeled peroxisomes, $\sim 94.7\%$ of End3p was localized to the peroxisome,

while the localization of the other proteins was partial (Ent1p, $\sim 64.0\%$; Ent2p, $\sim 66.7\%$; Sla1p, $\sim 63.3\%$; Sla2p, $\sim 72.0\%$; Fig. 5 E). Thus, it is likely that End3p and the other proteins interact with Pan1p by different mechanisms.

Since previous studies have reported that Pan1p and End3p form a stable complex with 1:1 stoichiometry (Sun et al., 2015a; Toshima et al., 2007), we speculated that End3p stably interacts with Pan1p at the peroxisome as well. Quantification of the End3-GFP's fluorescence intensity confirmed that End3p was constantly localized to the peroxisome (Fig. 6, A and B; and Fig. S2 B and Video 4). In contrast, the interaction between Pan1p and Sla1p has been reported to be negatively regulated by Ark1p/Prk1p (Zeng et al., 2001). Two-color analysis using GFP-tagged endocytic proteins and Pex-FRB-mCherry showed that localization of Sla1p and Ent1p at the peroxisome regularly cycles, in a similar manner to Abp1p, with

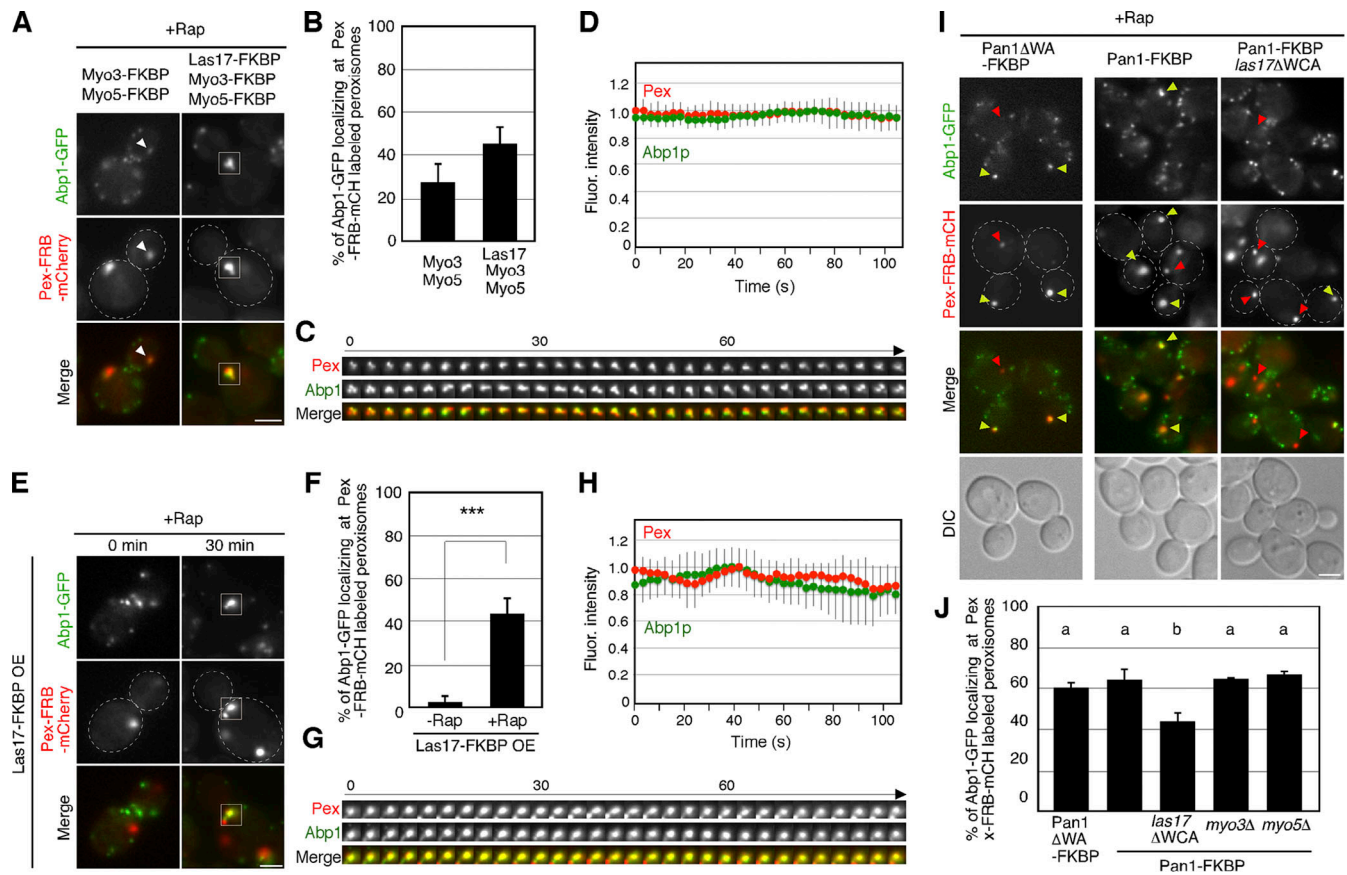


Figure 4. Las17p and Myo3p/5p cooperatively cause actin polymerization at the peroxisome. (A and E) The localization of Pex-FRB-mCherry and Abp1-GFP in cells expressing Las17-FKBP and/or Myo3/5-FKBP (A) or overexpressing Las17-FKBP (E). **(B, F, and J)** Quantification of the percentage of Abp1-GFP localizing at Pex-FRB-mCherry-labeled peroxisomes. Data show the mean \pm SD from three experiments ($n = 50$ puncta for each experiment). *******, P value < 0.001, unpaired t test with Welch's correction (F). Different letters indicate a significant difference between indicated times at $P < 0.001$, one-way ANOVA with Turkey's post-hoc test (J). **(C and G)** A time series of the boxed area is shown in the lower panels. **(D and H)** Averaged fluorescence intensities as a function of time for each protein ($n = 10$ independent peroxisomes). **(I)** The localization of Pex-FRB-mCherry and Abp1-GFP in cells expressing Pan1 Δ WA-FKBP, Pan1-FKBP, or Pan1-FKBP and Las17 Δ WCA at 30 min after rapamycin addition.

repeated appearance and disappearance at the peroxisome (Fig. 6, C and E; and Fig. S2, C and D; and Videos 5 and 6). Quantification of the fluorescence intensities of these proteins revealed that Sla1p and Ent1p showed a dynamic localization that increased gradually, and then decreased after reaching a maximum, similar to Abp1p (Fig. 6, D and F). Localization of Las17p or Myo3p was also found to change regularly, like Sla1p and Ent1p (Fig. S3, A–D), whereas the change in localization of Sla2p appeared to occur less regularly (Fig. S3, E and F), suggesting a distinct mechanism of localization for Sla2p. We also examined whether Sla2p, Ent1p, or Ent2p is conversely capable of recruiting Pan1p to the peroxisome when anchored to the latter, as these mid-coat proteins are reported to appear at endocytic sites before Pan1p (Weinberg and Drubin, 2012). To this end, we fused Sla2p, Ent1p and Ent2p to GFP and FKBP, and confirmed that these proteins were targeted to the peroxisome in the presence of rapamycin (Fig. S4, A–C). In contrast to the situation when Pan1p was anchored to the peroxisome, no Pan1p recruitment was observed when Sla2-, Ent1-, or Ent2-FKBP was thus anchored (Fig. S4, D–F). Furthermore, rapamycin treatment elicited no recruitment of Abp1p to the

peroxisome (Fig. S4, G–I). These results suggest that neither Sla2p, Ent1p, or Ent2p is able to recruit Pan1p and initiate actin polymerization by itself.

Finally, we examined the timing of recruitment of Sla1p and Abp1p, markers of late coat and actin polymerization, respectively, to the peroxisome. At the endocytic sites, Sla1p appeared ~ 10 – 15 s earlier than Abp1p, the intensity of Sla1p reached the maximum when Abp1p appeared at the site, and then Sla1p disappeared from the site before Abp1p (Kaksonen et al., 2005). Interestingly, triple-color live cell analysis showed that Sla1p and Abp1p behaved in a similar manner as at the endocytic site, where Sla1p appeared at the peroxisome first, and then Abp1p appeared when the fluorescence intensity of Sla1p approached the maximum (Fig. 6, G and H; and Fig. S2 E and Video 7). These data suggest that Pan1p regulates the assembly of the endocytic machinery required for the mid-to-late stage of endocytosis and also regulates its disassembly.

Effect of ectopic targeting of Pan1p to mitochondria on localization of endocytic proteins

We have shown that localization of mid- and late-coat proteins depend on Pan1p by ectopically localizing Pan1p to the

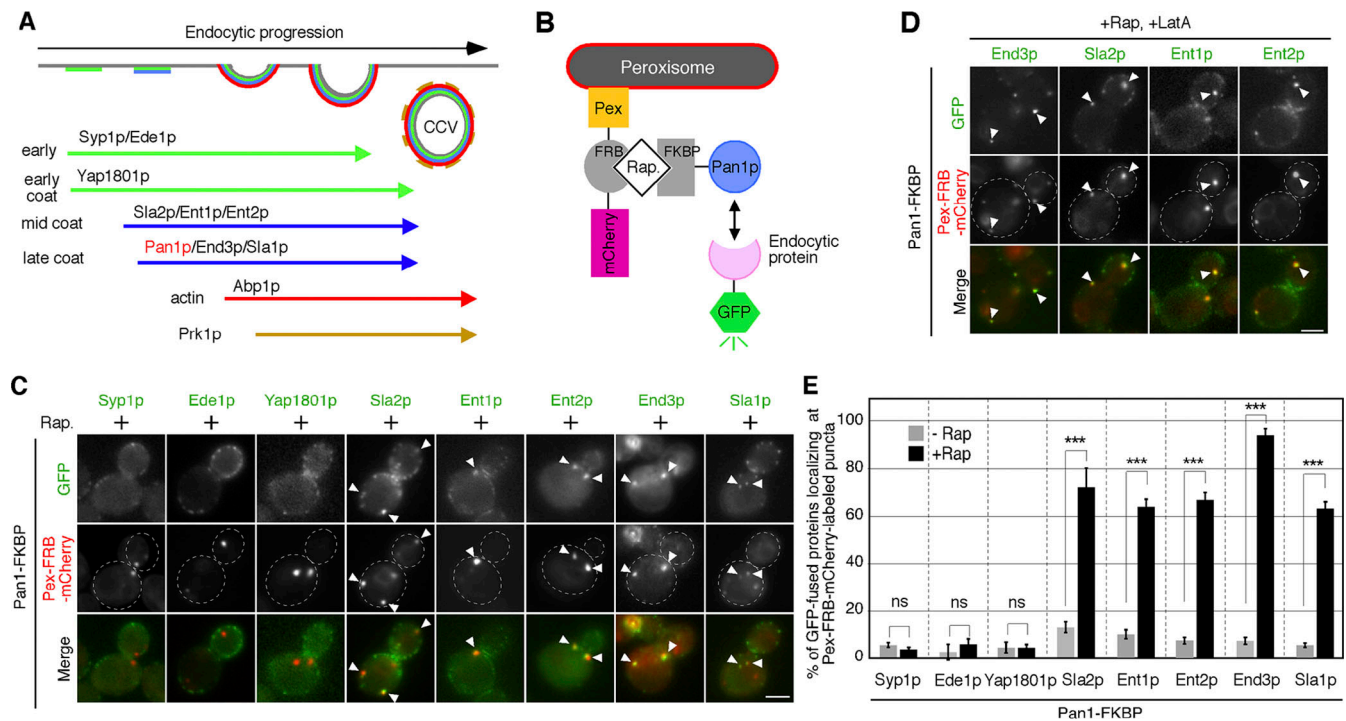


Figure 5. Ectopically localized Pan1p can recruit the mid- and late-coat proteins to the peroxisome. (A) Spatial-temporal recruitment of endocytic proteins. Timing of appearance and disappearance of endocytic proteins at the endocytic site are shown below. (B) Schematic diagrams of the inducible peroxisome redistribution assay. (C) Localization of GFP-tagged endocytic proteins and Pex-FRB-mCherry at 30 min after rapamycin addition. White arrowheads indicate examples of co-localization. (D) Localization of GFP-tagged endocytic proteins and Pex-FRB-mCherry at 30 min after rapamycin addition in the presence of 200 μ M LatA. (E) Quantification of the percentage of the indicated GFP-tagged endocytic proteins localizing at Pex-FRB-mCherry-labeled peroxisomes before and after Rapamycin addition. Data show the mean \pm SD from three experiments ($n = 50$ puncta for each experiment). ***, P value < 0.001 , unpaired t test with Welch's correction. Scale bars, 2.5 μ m.

peroxisomes. We next wished to determine the extent to which the localization of each endocytic protein to the actual endogenous endocytic site is dependent on Pan1p. We first targeted Pan1-FKBP to peroxisomes and examined the effect on Pan1p localization at cortical patches. While most Pan1p changed its localization to the peroxisome, $\sim 24\%$ still remained localized at the cortical patches (Fig. S5 A). To remove Pan1p from endocytic sites more efficiently, we next utilized Mito-mCherry-FRB, a fusion protein containing the mitochondrial outer membrane protein OM45 coupled to mCherry and FRB, to anchor Pan1p to mitochondria (Fig. 7 A). At 30 min after the addition of rapamycin, in cells expressing Mito-FRB-mCherry, Pan1-GFP-FKBP changed its localization to the mitochondria (Fig. 7 B), with only $\sim 0.8\%$ of the Pan1p present at cortical patches before addition (Fig. 7 C). Since Pan1p is essential for endocytosis, its removal from the endocytic site should severely impair endocytosis. To confirm this, we labeled cells expressing Pan1-FKBP and Mito-mCherry-FRB with Alexa Fluor 594-labeled α -factor (A594- α -factor; Toshima et al., 2006) in the presence or absence of rapamycin and followed the localization at several time points after α -factor internalization. As expected, in rapamycin-untreated cells the majority of A594- α -factor was transported to the vacuole after 20 min, whereas an obvious delay of α -factor internalization was observed in rapamycin-treated cells (Fig. 7, D and E). Similar to the situation when Pan1p was targeted to the peroxisome and when Pan1p was

targeted to mitochondria, the mid- and late-coat proteins exhibited localization at mitochondria, but localization of early or early coat proteins was not observed (Fig. 7 F; and Fig. S5, B and C). To test if the recruitment of Pan1-FKBP causes tethering of endocytic vesicles to mitochondria, we again examined the localization of FM4-64 and found that FM4-64-labeled puncta were rarely observed at mitochondria in the presence of rapamycin although Abp1p is recruited there (Fig. S5 D). Consistent with this localization at the mitochondria, in cells treated with rapamycin, the fluorescence intensities of the mid or late coat proteins at cortical patches were significantly decreased, whereas those of early or early coat proteins were not affected (Fig. 7, F and G). The fluorescence intensity of End3-GFP at cortical patches decreased to a similar level ($\sim 1.3\%$) as that of Pan1-GFP (Fig. 7, C, F and G), indicating that most End3p was targeted to mitochondria by forming a stable complex with Pan1p. The marked decrease of Sla1-GFP localization at cortical patches ($\sim 33.9\%$) also suggested that Sla1p is a major binding partner of Pan1p (Fig. 7, F and G), consistent with previous findings (Tang et al., 2000). As Abp1p localizes to cortical patches dependent on actin filaments, more Abp1p may reroute to mitochondria where Pan1p-dependent ectopic actin polymerization occurs (Fig. 7, F and G). Intriguingly, contrary to previous observations (Bradford et al., 2015; Sun et al., 2015a), localization of the mid-coat proteins Ent1p, Ent2p, and Sla2p was also partially affected by ectopic targeting of Pan1p to mitochondria (Fig. 7, F and G).

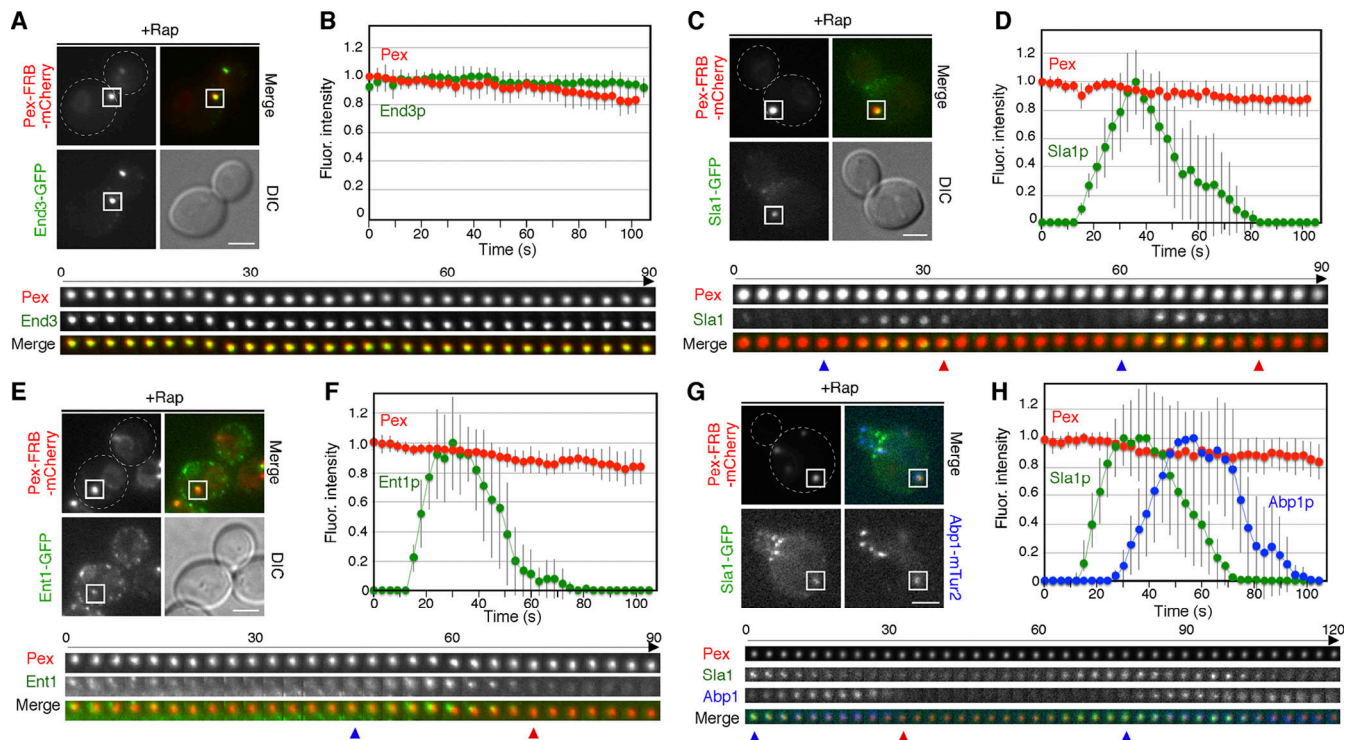


Figure 6. Dynamic localization of endocytic proteins at Pan1p-anchoring peroxisomes. (A, C, and E) The localization of Pex-FRB-mCherry and GFP-fused End3p (A), Sla1p (C), or Ent1p in cells expressing Pan1-FKBP at 30 min after rapamycin addition. The upper panels show single frames from movies of the indicated strain. A time series of the boxed area is shown in the lower panels. Blue or red arrowheads indicate the timing of the appearance or disappearance respectively of GFP signal. Quantification of fluorescence intensities for each protein in the boxed area is shown in Fig. S2, B–D. (B, D, and F) Averaged fluorescence intensities as a function of time for each protein ($n = 10$ independent peroxisomes). (G) The localization of Sla1-GFP, Abp1-mTur2, and Pex-FRB-mCherry in cells expressing Pan1-FKBP at 30 min after rapamycin addition. A time series of the boxed area is shown in the lower panels. Quantification of fluorescence intensities for each protein in the boxed area is shown in Fig. S2 E. (H) Averaged fluorescence intensities as a function of time for each protein ($n = 10$ independent peroxisomes). Scale bars, 2.5 μm .

Actin assembly by the Pan1p complex recruits Prk1p and cofilin, leading to actin depolymerization and disassembly of the endocytic machinery

We demonstrated that at Pan1p-anchoring peroxisomes, the mid/late coat proteins, and Abp1p appear periodically and then disappear in a manner similar to the dynamics observed at sites of endocytosis (Fig. 6, G and H), suggesting that endocytic coat disassembly and subsequent actin depolymerization occur regularly at the peroxisome. This motivated us to further examine the localization of proteins such as Prk1p, cofilin (Cof1p), and Srv2p, which regulate endocytic coat disassembly and actin depolymerization (Fig. 8 A). To this end, we fused GFP to these proteins and expressed them in a strain expressing Pex-FRB-mCherry and Pan1-FKBP (Fig. S5 E). As expected, we found that ~40% of Prk1p became localized at peroxisomes after the addition of rapamycin (Fig. 8, B and C; and Video 8), and that this localization was remarkably inhibited by LatA treatment (Fig. S5 F). To determine the timing of Prk1p recruitment to the peroxisome, we compared the dynamics of Abp1-mTurquoise2 (mTur2) and Prk1-GFP in cells anchoring Pan1p to the peroxisome. Triple-color imaging demonstrated that Prk1p recruitment to the peroxisome was slightly delayed in relation to Abp1p (Fig. 8 D), similar to Prk1p dynamics at the endocytic site (Toret et al., 2008). This suggested that Pan1p might be phosphorylated

by Prk1p at the peroxisome, as well as at the endocytic site, resulting in disassembly of the mid/late coat proteins and actin. We also found that the actin depolymerization factor Cof1p, and Srv2p, which cooperatively accelerates actin depolymerization with Cof1p, were recruited to the peroxisome (~51.0 or ~52.6%, respectively; Fig. 8, E, G, H, and J; and Videos 9 and 10). Triple-color imaging using Abp1-mTur2 and Cof1-GFP or Srv2-GFP revealed that these proteins were recruited to the peroxisome several seconds after Abp1p recruitment and reached their maximum fluorescence intensities after Abp1p (Fig. 8, E, F, H, and I). Thus, Cof1p and Srv2p are likely to regulate the disassembly of the actin cytoskeleton assembled by the Pan1p complex at peroxisomes.

Pan1p recruits actin cables to the peroxisome

In addition to the role of Pan1p in CCV formation, Pan1p is also reported to regulate the interaction between endocytic vesicles and actin cables (Toshima et al., 2016; Toshima et al., 2006). Accordingly, we next examined whether actin cables interact with peroxisomes when Pan1p is anchored there. To this end, we labeled actin cables with triple GFP (3GFP)-tagged Abp140p and examined the spatiotemporal relationship between Pan1p-anchoring peroxisomes and actin cables. In the absence of rapamycin, little interaction between

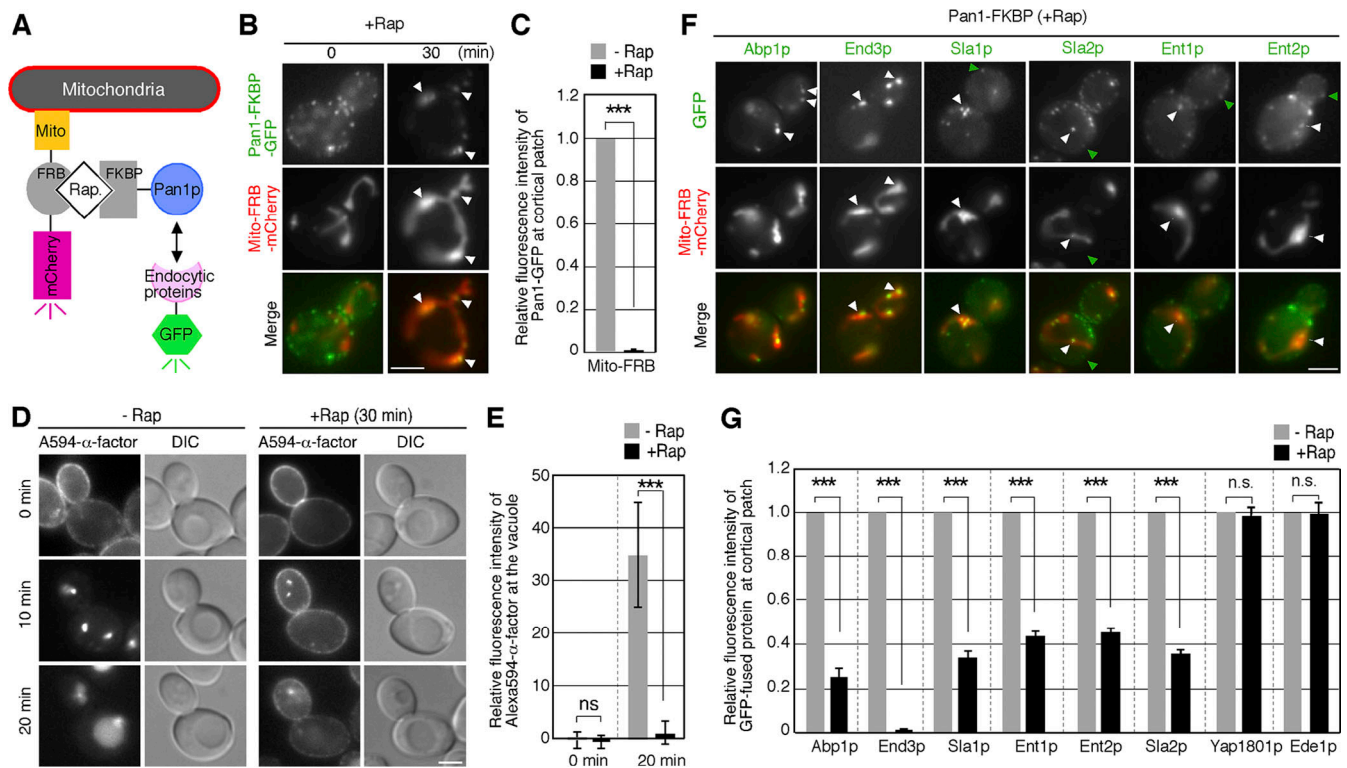


Figure 7. Effect of anchoring Pan1p to the mitochondria on localization of endocytic proteins at endocytic sites. (A) Schematic diagrams of the inducible mitochondria redistribution assay. (B) Each image pair was acquired before or at 30 min after rapamycin addition. White arrowheads indicate examples of co-localization. (C) Relative fluorescence intensity of Pan1p at cortical patches in cells anchoring Pan1p to the mitochondria. Data show the mean \pm SEM from three experiments ($n = 30$ patches for each experiment). ***, P value < 0.001 , unpaired t test with Welch's correction. (D) Transport of A594- α -factor in cells anchoring Pan1p to the mitochondria. Cells were labeled with A594- α -factor in the presence or absence of rapamycin, and the images were acquired at 0, 10, and 20 min after washing out unbound A594- α -factor and inducing internalization. (E) Relative fluorescence intensity of vacuoles stained by A594- α -factor. Data show the mean \pm SD from three experiments ($n = 30$ for each experiment). Values were relative to the fluorescence intensity in cells after 20 min. (F) Localization of GFP-tagged endocytic proteins and Mito-FRB-mCherry at 30 min after rapamycin addition. White arrowheads indicate examples of co-localization and green arrowheads examples of GFP-tagged proteins localizing at cortical patches. (G) Quantification of relative fluorescence intensity of GFP-fused endocytic proteins at cortical patches. The bar graphs represent the relative intensities of GFP-tagged protein after rapamycin addition, compared with those before rapamycin addition. Data show the mean \pm SEM from three experiments ($n = 30$ patches for each experiment). ***, P value < 0.001 , **, P value < 0.01 , ns, non-statistically significant, unpaired t test with Welch's correction. Scale bars, 2.5 μ m.

peroxisomes and actin cables was observed ($\sim 4.3\%$), but the interaction increased markedly after rapamycin addition ($\sim 47.0\%$; Fig. 9, A–C; and Video 11). Interestingly, we observed Pan1p-anchored peroxisomes transiently interacting with and moving along actin cables, labeled by Abp140-3GFP, when actin assembly was initiated at the peroxisome (Fig. 9 A). Then, the peroxisome dissociated from the actin cable at almost the same time point as actin disassembly (Fig. 9 A, lower panels). In contrast, such peroxisome dynamics along actin cables were rarely observed in the absence of rapamycin (Fig. 9 B). Quantification of peroxisome velocity revealed that in the presence of rapamycin, peroxisomes move on actin cables with an average speed of $217.6 \pm 83.7 \mu\text{m/s}$, whereas peroxisomes in the absence of rapamycin move little ($36.9 \pm 18.6 \mu\text{m/s}$; Fig. 9 D). This movement of peroxisomes closely resembles that of endocytic vesicles, which move on actin cables when being internalized into the cell (Huckaba et al., 2004; Toshima et al., 2006). These findings suggest that the Pan1p complex directly regulates the interaction between endocytic vesicles and actin cables.

Discussion

Pan1p serves as a master regulator of the late stage of the endocytic pathway

Clathrin-mediated endocytosis is driven by sequential assembly and disassembly of numerous endocytic proteins at the plasma membrane. The timing of the appearance and behavior of these proteins at endocytic sites has been well characterized (Goode et al., 2015; Kaksonen and Roux, 2018; Weinberg and Drubin, 2012), but the molecular mechanisms whereby endocytic proteins are recruited have remained unclear. One particularly important issue remaining to be clarified has been the manner in which mid/late coat proteins are recruited to endocytic sites because in cells lacking most of the genes encoding early-phase proteins, the mid/late coat proteins are regularly recruited to endocytic sites and the dynamics of vesicle budding are largely normal (Brach et al., 2014). In the present study, we showed that Pan1p anchored to the peroxisome was capable of initiating all of the events occurring at the late stage of endocytosis, including mid/late coat protein recruitment, NPF-mediated actin polymerization, coat and actin

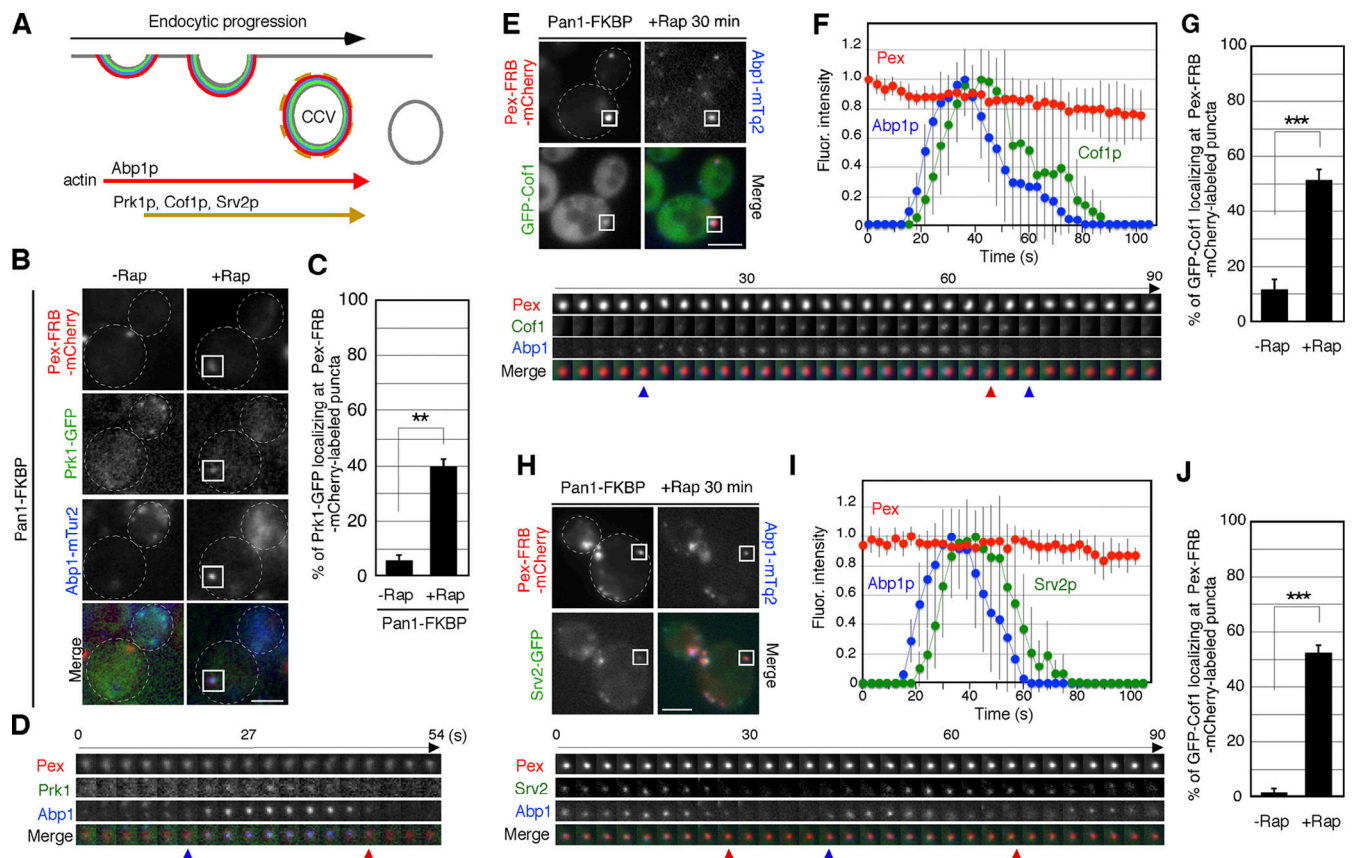


Figure 8. Dynamic localization of actin disassembly factors at Pan1p-anchoring peroxisomes. (A) Spatial-temporal recruitment of Prk1p, Cof1p, and Srv2p. Timing of appearance and disappearance of actin disassembly factors are shown below. (B) Localization of Prk1-GFP, Pex-FRB-mCherry, and Abp1-mTur2 before or at 30 min after rapamycin addition. (C) Quantification of the percentage of Prk1-GFP localizing at Pex-FRB-mCherry-labeled puncta. Data show the mean \pm SD from three experiments ($n = 50$ puncta for each experiment). (D) The time series of each protein in the boxed area in B are shown. Blue or red arrowheads indicate the timing of the appearance or disappearance of Abp1-CFP signal. (E and H) The localization of GFP-Cof1 (E) or Srv2-GFP (H), Abp1-mTur2, and Pex-FRB-mCherry at 30 min after rapamycin addition. A time series of a single peroxisome in the boxed area is shown in the lower panels. Blue or red arrowheads indicate the timing of the appearance or disappearance of the indicated fusion protein's signal. (F and I) Averaged fluorescence intensities as a function of time for each protein ($n = 10$ independent peroxisomes). (G and J) Quantification of the percentages of GFP-Cof1 (G) or Srv2-GFP (J) localizing at Pex-FRB-mCherry-labeled peroxisomes before and after rapamycin addition. Throughout figure blue or red arrowheads indicate the timing of the appearance or disappearance of the indicated fusion protein's signal. Data show the mean \pm SD from three experiments ($n = 100$ puncta for each experiment). **, P value < 0.01 , ***, P value < 0.01 , unpaired t test with Welch's correction. Scale bars, 2.5 μ m.

disassembly, and actin cable recruitment at the peroxisome (Fig. 10). These findings suggest that Pan1p serves as a master regulator of the late stage of endocytosis.

How is actin assembly regulated at endocytic sites?

A transient burst of actin polymerization and subsequent depolymerization at the endocytic site is required for the formation and internalization of a CCV (Kaksonen et al., 2003; Merrifield et al., 2002). Previous studies have reported that mutant Las17p, which lacks the ability to activate the Arp2/3 complex, causes a severe defect of actin polymerization at endocytic sites. In contrast, it has been demonstrated that mutant forms of Pan1p and Myo3p/5p which lack Arp2/3 activation capability do not significantly affect actin polymerization (Sun et al., 2006). These observations suggested that the NPF activity of Las17p plays a central role in the initiation of actin polymerization at endocytic sites, while Pan1p has only an auxiliary role. In the present study, however, we showed that

anchoring of Las17p to the peroxisome elicited little actin polymerization in situ, whereas anchoring of Pan1p was sufficient to trigger substantial actin polymerization. Consistent with this observation, previous studies reported that in cells lacking full-length Pan1p by the auxin-inducible degron system, actin polymerization at endocytic sites was severely defective, and the number of cortical patches was significantly decreased (Bradford et al., 2015; Sun et al., 2015a). These suggested that the function of Pan1p as a scaffold protein, in addition to the NPF activity, is important for accumulating all NPFs in a particular region and initiating explosive actin polymerization at the endocytic site.

A recent study has shown that the accumulation of Las17p and Myo3p above a certain threshold at endocytic sites triggers actin polymerization and that the Pan1p complex is implicated in the regulation of that process (Sun et al., 2017). Pan1p anchored to the peroxisome likely recruits Las17p and Myo3p/5p in a similar manner as at the endocytic site, causing accumulation of these

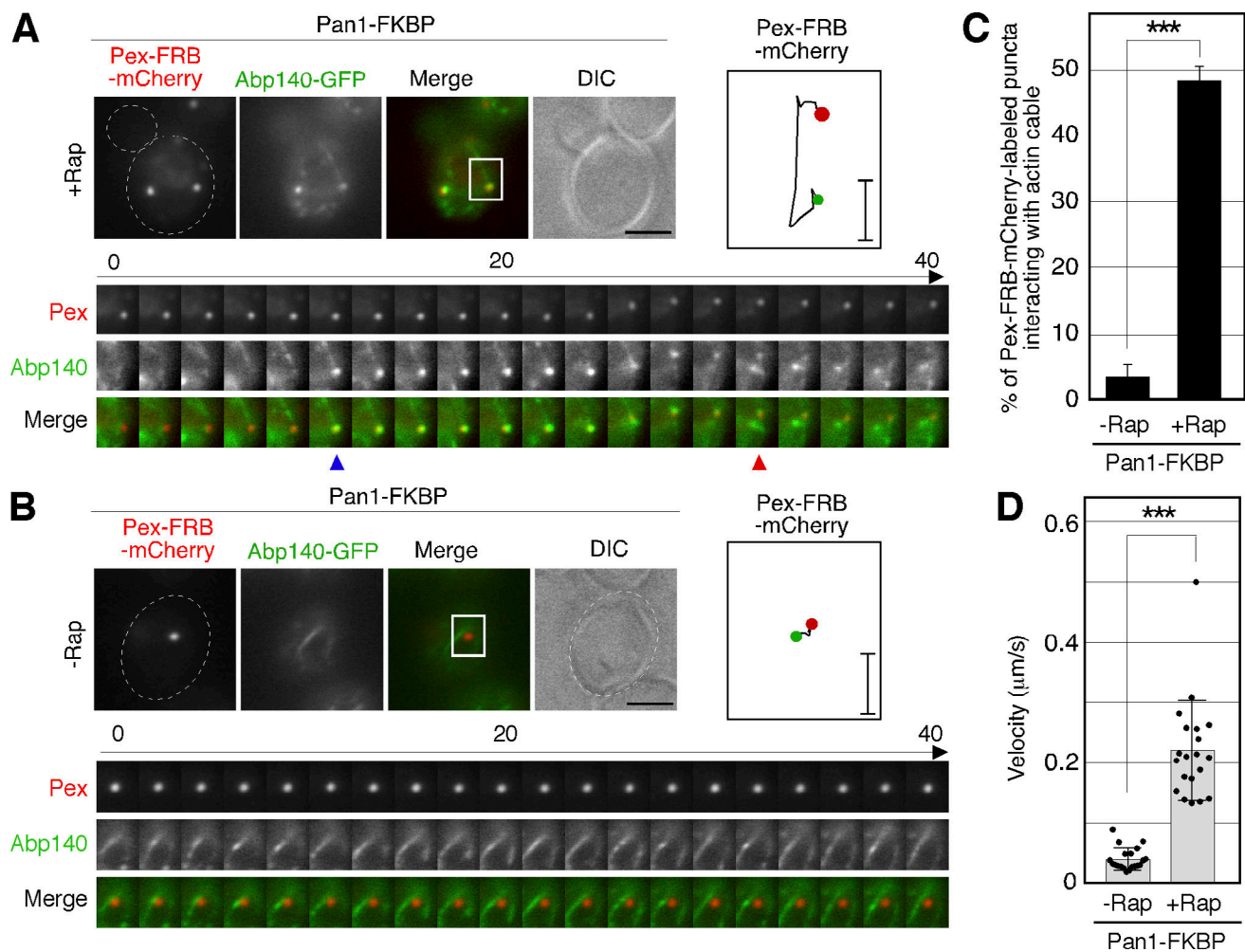


Figure 9. Pan1p recruits actin cable to the peroxisome. (A and B) Localization of Abp140-GFP and Pex-FRB-mCherry (A) after or (B) before rapamycin addition. In the upper row the left two panels show the individual channels and the right two panels show the merged image and DIC image. The time series of each protein in the boxed area is shown in the lower panels. Blue or red arrowheads indicate the timing of association or dissociation of the peroxisome and actin cable. Tracking of Pex-FRB-mCherry-labeled peroxisome in the boxed area. Green and red dots denote the first and last positions, respectively, of each peroxisome. Scale bars, 400 nm. **(C)** Quantification of the percentage of Pex-FRB-mCherry-labeled peroxisomes that interact with actin cables in the presence of Pan1-FKBP before and after rapamycin addition. Data show the mean \pm SD from at least three experiments ($n = 50$ puncta for each experiment). **(D)** Quantification of the velocity of Pex-FRB-mCherry-labeled peroxisomes that interact with actin cables before and after rapamycin addition. Data show the mean \pm SD ($n = 20$ puncta for each experiment). ***, P value < 0.001 , unpaired t test with Welch's correction.

NPFs to the peroxisome. On the other hand, anchoring of Las17p or Myo3p/5p alone might not recruit sufficient NPFs to initiate actin polymerization. Taken together, these findings suggest that Pan1p likely accumulates the actin assembly machinery at endocytic sites and generates the force for CCV formation and invagination through intensive polymerization of actin.

Pan1p recruits the mid/late coat proteins and mediates the later stage of endocytosis

Previous studies demonstrated that Pan1p possesses multiple functional regions, such as two EH domains in the N-terminal region, a central coiled-coil region, and actin and Arp2/3 binding regions in the C-terminal region (Toshima et al., 2005; Wendland and Emr, 1998), and forms complexes with various endocytic proteins. However, it has not been definitively identified which proteins, especially early and mid-coat proteins,

Pan1p interacts directly with *in vivo*. The EH domains are reported to interact with NPF motifs in Yap1801p/2p and Ent1p/2p, which are early and mid-coat proteins (Suzuki et al., 2012; Wendland and Emr, 1998; Wendland et al., 1999). However, our analysis showed that Pan1p was not capable of recruiting Yap1801p/2p to the peroxisome, and that localization of Yap1801p/2p was not affected even when most of the Pan1p was targeted to mitochondria. Similarly, localization of Yap1801p/2p was not affected in cells depleted of Pan1p (Bradford et al., 2015), suggesting that Yap1801p/2p, rather than Pan1p, might preferentially interact with components in the early clathrin coat (Huang et al., 1999). In contrast, Pan1p was able to recruit the mid-coat proteins Ent1p/2p and Sla2p, which contain the ANTH/ENTH domains that interact specifically with phosphoinositides (Legendre-Guillemin et al., 2004). These proteins are reported to be normally localized at cortical patches in cells depleted of

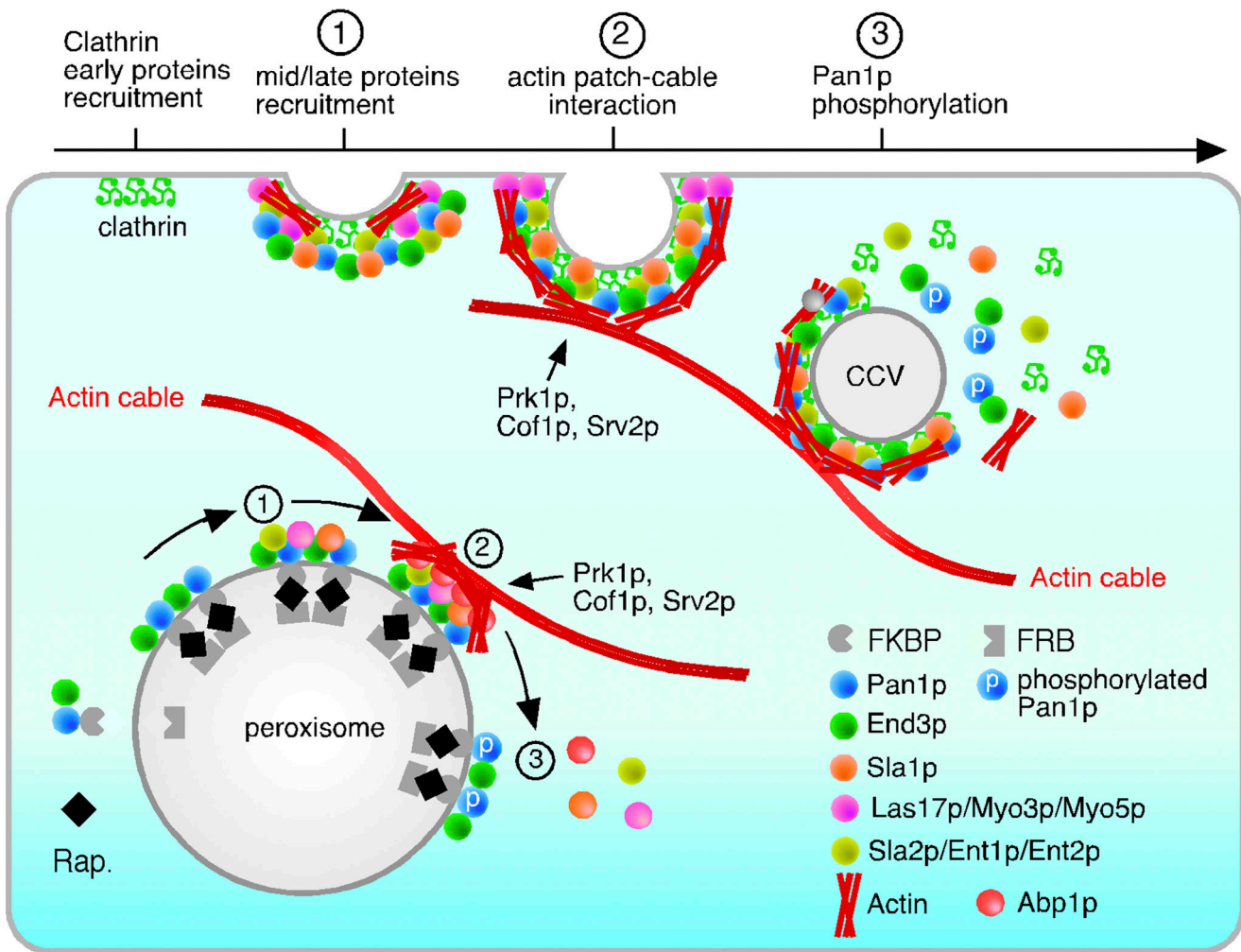


Figure 10. **Model of the Pan1p-mediated recruitment of endocytic proteins and actin.** FKBP-tagged Pan1p makes a stable complex with End3p and becomes anchored at the peroxisome upon rapamycin addition. Pan1p recruits the mid/late coat proteins to the peroxisome and leads to actin polymerization. As actin polymerization is initiating, the peroxisome attaches to and moves on an actin cable. Once actin polymerization begins, Prk1p and actin disassembly factors, such as Cof1p and Srv2p, are recruited to the peroxisome and disassemble the coat complex and actin cytoskeleton. We posit that the same sequence of events happens at normal endocytic sites upon the recruitment of Pan1 by an as-yet-unknown triggering event.

Pan1p (Bradford et al., 2015; Sun et al., 2015a); however in our analysis, their localization at cortical patches is decreased when Pan1p was targeted to mitochondria, as it partially reroutes these proteins to mitochondria. This observation suggests that Pan1p or the Pan1p complex directly interacts with these mid coat proteins, thereby being recruited to the endocytic site and progressing to later stages of the endocytic pathway.

Interaction between Pan1p and several endocytic proteins is regulated by the Pan1p phosphorylation cycle (Smythe and Ayscough, 2003), but previous studies have failed to demonstrate which interactions are phosphorylation-dependent in vivo because the Pan1p complex disappears from the cortical patch when the endocytic vesicle is internalized (Kaksonen et al., 2003). Our analysis clearly demonstrated which proteins stably or transiently interacted with Pan1p in vivo. End3p has been shown to interact stably with Pan1p (Sun et al., 2015b; Toshima et al., 2007), and this was also confirmed in the present analysis. Interaction of Sla1p and Ent1p with Pan1p is reported to be regulated by phosphorylation

(Watson et al., 2001; Zeng et al., 2001), and our present analysis also showed that it is periodically regulated. Interestingly, the interaction between Pan1p and Las17p or Myo3p/5p appeared to be regulated by the Pan1p phosphorylation cycle. Since these interactions are mediated by Sla1p (Feliciano and Di Pietro, 2012; Rodal et al., 2003), phosphorylation-dependent dissociation of Sla1p from Pan1p could also cause dissociation of these proteins.

Pan1p regulates the disassembly of the actin cytoskeleton during endocytosis

Important regulators of actin disassembly are the Ark1p/Prk1p kinases (Smythe and Ayscough, 2003). Among the many substrates for Ark1p/Prk1p kinases, Pan1p is the major in vivo substrate, as *pan1*, mutated to prevent phosphorylation at all 18 threonines (*pan1-18TA*), displays almost the same endocytic defect as *ark1Δ prk1Δ* cells (Toshima et al., 2016). Recruitment of these kinases to sites of endocytosis depends on Abp1p (Cope et al., 1999), and is delayed relative to Abp1p recruitment by

1–2 s (Toret et al., 2008). This timing of Prk1p recruitment is almost coincident with that at the Pan1p-anchoring peroxisome and the timing of Pan1p complex disassembly there. Thus, one potential model that can be considered is that at both peroxisomes and endocytic sites, Pan1p triggers actin assembly, which in turn recruits Abp1p, and Ark1/Prk1 kinases are then recruited in an Abp1p-dependent manner to phosphorylate Pan1p, resulting in the dissociation of the actin filament from Pan1p.

Cof1p and Srv2p enhance actin disassembly by binding around the pointed ends of actin filaments, which have abundant ADP-actin (Balcer et al., 2003). Abp1p also mediates the recruitment of Srv2p to cortical patches (Freeman et al., 1996; Lila and Drubin, 1997). Our present analysis showed that these proteins were also recruited to the Pan1p-anchoring peroxisome, suggesting that Cof1p and Srv2p function cooperatively with Ark1/Prk1 kinases to facilitate rapid actin disassembly. Clathrin coat disassembly is regulated by the lipid phosphatase Sjl2p and recruitment of Sjl2p to endocytic sites is dependent on Abp1p (Stefan et al., 2005). Thus, Sjl2p could be similarly recruited to the Pan1p-anchoring peroxisome and regulates the disassembly of the endocytic machinery.

Materials and methods

Yeast strains, growth conditions, and plasmids

The yeast strains used in this study are listed in Table S1. All strains were grown at 25°C in standard rich medium (YPD) or synthetic medium (SM) supplemented with 2% glucose and appropriate amino acids. For rapamycin-induced heterodimerization of FRB and FKBP 10 μ M, rapamycin was added to cultures 15 or 30 min before imaging. The GFP-FKBP- or FKBP-tagged proteins were expressed as follows: the NotI-SacII fragment, which contains the *S. cerevisiae* ADHI terminator (TADHI) and the URA3MX6 module, was amplified by PCR using pFA6a-mCherry-URA3MX6 (Kawada et al., 2015) as a template and inserted into NotI- and SacII-digested pBS-GFP (pBS-TADHI-URA3). The NotI-SacII fragment containing GFP-FKBP or FKBP was amplified by PCR using GFP-FKBP-LCa plasmid (#59353; Addgene) as a template and inserted into BamHI- and NotI-digested pBS-TADHI-URA3 (pBS-GFP-FKBP-TADHI-URA3 or pBS-FKBP-TADHI-URA3). To create integration vectors, the C-terminal fragment of Pan1 (nt 3608–4440), Sla2 (nt 2231–2904), Ent1 (nt 634–1362), Ent2 (nt 634–1362), Las17 (nt 1021–1888), Myo3 (nt 3481–3816), or Myo5 (nt 3661–3957) was amplified by each primer set listed in Table S2, digested with BamHI or BglII, and inserted into BamHI-digested pBS-GFP-FKBP-TADHI-URA3 or pBS-FKBP-TADHI-URA3. To integrate the C-terminal GFP-FKBP or FKBP tag at the endogenous of the target gene, the integration plasmid for Pan1, Sla2, Ent1, Ent2, Las17, Myo3, or Myo5 was linearized by EcoNI, MfeI, MfeI, AflII, EcoRV, SpeI, or EcoRI, respectively, and transformed into JTY9191. Pex-mCherry-FRB or Mito-mCherry-FRB was expressed as follows: pRS305 containing the *S. cerevisiae* TPPII promoter (PTPII) and STE2 terminator (TSTE2) was created by inserting the SacI-XhoI fragment of PTPII-(BamHI)-TSTE2 extracted from pRS316-PTPII-(BamHI)-TSTE2 plasmid (Abe et al., 2019) into BamHI site of pRS305 (pRS305-PTPII-(BamHI)-TSTE2). The N-terminal fragment of Pex3p (nt1–135; Pex) was amplified

by PCR with JT3556 and JT3674 using yeast genome DNA as a template, and the mCherry-FRB fragment (mCherry-FRB) was amplified by PCR with JT3675 and JT3291 using pMito-mCherry-FRB plasmid (#59352; Addgene) as a template. Next, the Pex-mCherry-FRB fragment was amplified by PCR with JT3556 and JT3291 using Pex and mCherry-FRB fragments as the template and inserted into the BamHI site of pRS305-PTPII-TSTE2 (pRS305-PTPII-Pex-FRB-mCherry-TSTE2). To create Mito-mCherry-FRB integration plasmid, the BglII fragment containing Mito-mCherry-FRB was amplified by PCR using pMito-mCherry-FRB plasmid (#59352; Addgene) as a template and inserted into BamHI site of pRS305-PTPII-TSTE2 (pRS305-PTPII-Mito-mCherry-FRB-TSTE2). To integrate these plasmids into the endogenous locus of the *HIS3* gene, the plasmids were linearized by EcoRV and transformed into yeast.

Fluorescence labeling of α -factor and endocytosis assays

3-Thiopropionyl-G₃ was appended to the free ϵ -amine of K₇ in otherwise fully-protected α -factor by standard DCC/HOBT FMOc solid phase chemistry, and Alexa-594 maleimide (Thermo Fisher Scientific) was coupled to the purified peptide in NMM-HOAc buffer, pH 8.0. Peptides were purified by reverse-phase HPLC; structure and purity (>95%) were assessed by ESI-FTICR mass spectrometry. For endocytosis assays, cells were grown to an OD₆₀₀ of ~0.5 in 0.5 ml YPD, briefly centrifuged, and re-suspended in 20 μ l SM with 5 μ M Alexa Fluor-labeled α -factor. After incubation on ice for 2 h, the cells were washed with ice-cold SM. Internalization was initiated by the addition of SM containing 4% glucose and amino acids at 25°C.

Fluorescence microscopy

Fluorescence microscopy was performed using an Olympus IX83 microscope equipped with a \times 100/NA 1.40 (Olympus) or a \times 100/NA 1.49 (Olympus) objective and Orca-AG cooled CCD camera (Hamamatsu) using Metamorph software (Universal Imaging). Triple color imaging was performed using an Olympus IX81 microscope equipped with a high-speed filter changer (Lambda 10-3; Shutter Instruments) that can change filter sets within 40 ms. All cells were imaged during the early- to mid-logarithmic phase.

Statistics

Statistical analysis was conducted using Prism 7 (GraphPad Software). Significance was tested by a two-sided Student's *t* test for two-group comparisons or ANOVA with Turkey's post-hoc test as specified in the figure legends for comparisons of three or more groups.

Online supplemental material

Fig. S1 shows targeting of Pan1p to the peroxisome leads to actin polymerization by recruiting other NPFs. Fig. S2 shows localization and fluorescence intensity of endocytic proteins at Pan1p-anchoring peroxisomes. Fig. S3 shows dynamic localization of endocytic proteins at Pan1p-anchoring peroxisomes. Fig. S4 shows ectopically localized Ent1p, Ent2p, and Sla2p cannot recruit Pan1p. Fig. S5 shows localization of endocytic proteins in cells expressing Pan1-FKBP and Mito-FRB-mCherry, and actin-

dependent recruitment of Prk1-GFP to the Pan1p-anchoring peroxisome. Table S1 shows yeast strains used in this study. Table S2 lists primers used in this study. Data S1 contains source data for LatA treatment and recovery in Fig. 1 F. Video 1 shows de novo synthesis of F-actin at Pan1p-anchoring peroxisome. Video 2 shows Arp2/3-dependent actin assembly at Pan1p-anchoring peroxisome. Video 3 shows dynamics of Pan1-GFP and Abp1-CFP at Pan1p-anchoring peroxisome. Video 4 shows dynamics of End3-GFP at Pan1p-anchoring peroxisome. Video 5 shows dynamics of Sla1-GFP at Pan1p-anchoring peroxisome. Video 6 shows dynamics of Ent1-GFP at Pan1p-anchoring peroxisome. Video 7 shows dynamics of Sla1-GFP and Abp1-mTq2 at Pan1p-anchoring peroxisome. Video 8 shows dynamics of Prk1-GFP and Abp1-mTq2 at Pan1p-anchoring peroxisome. Video 9 shows dynamics of GFP-Cof1 and Abp1-mTq2 at Pan1p-anchoring peroxisome. Video 10 shows dynamics of Srv2-GFP and Abp1-mTq2 at Pan1p-anchoring peroxisome. Video 11 shows recruitment of actin cable to Pan1p-anchoring peroxisome.

Acknowledgments

This work was supported by JSPS KAKENHI GRANT #18K062291, and the Takeda Science Foundation to J.Y. Toshima, as well as JSPS KAKENHI GRANT #19K065710, the Uehara Memorial Foundation, and Life Science Foundation of JAPAN to J. Toshima.

The authors declare no competing financial interest.

Author contributions: M. Enshoji, Y. Miyano, N. Yoshida, M. Watanabe, and M. Kunihiro: Investigation, Data curation. M. Nagano: Investigation, Data curation, Project administration, D.E. Siekhaus: Writing-Review and Editing. J.Y. Toshima: Investigation, Data curation, Funding acquisition, Supervision. J. Toshima: Supervision, Conceptualization, Funding acquisition, Writing-original draft, Writing-Review and Editing.

Submitted: 29 December 2021

Revised: 30 June 2022

Accepted: 3 August 2022

References

Abe, M., M. Saito, A. Tsukahara, S. Shiokawa, K. Ueno, H. Shimamura, M. Nagano, J.Y. Toshima, and J. Toshima. 2019. Functional complementation reveals that 9 of the 13 human V-ATPase subunits can functionally substitute for their yeast orthologs. *J. Biol. Chem.* 294:8273–8285. <https://doi.org/10.1074/jbc.RA118.006192>

Anderson, B.L., I. Boldogh, M. Evangelista, C. Boone, L.A. Greene, and L.A. Pon. 1998. The Src homology domain 3 (SH3) of a yeast type I myosin, Myo5p, binds to verprolin and is required for targeting to sites of actin polarization. *J. Cell Biol.* 141:1357–1370. <https://doi.org/10.1083/jcb.141.6.1357>

Balcer, H.I., A.L. Goodman, A.A. Rodal, E. Smith, J. Kugler, J.E. Heuser, and B.L. Goode. 2003. Coordinated regulation of actin filament turnover by a high-molecular-weight Srv2/CAP complex, cofilin, profilin, and Aip1. *Curr. Biol.* 13:2159–2169. <https://doi.org/10.1016/j.cub.2003.11.051>

Banaszynski, L.A., C.W. Liu, and T.J. Wandless. 2005. Characterization of the FKBP center dot Rapamycin center dot FRB ternary complex. *J. Am. Chem. Soc.* 127:4715–4721. <https://doi.org/10.1021/ja043277y>

Brach, T., C. Godlee, I. Moeller-Hansen, D. Boeke, and M. Kaksonen. 2014. The initiation of clathrin-mediated endocytosis is mechanistically highly flexible. *Curr. Biol.* 24:548–554. <https://doi.org/10.1016/j.cub.2014.01.048>

Bradford, M.K., K. Whitworth, and B. Wendland. 2015. Pan1 regulates transitions between stages of clathrin-mediated endocytosis. *Mol. Biol. Cell.* 26:1371–1385. <https://doi.org/10.1091/mbc.E14-11-1510>

Cope, M.J., S. Yang, C. Shang, and D.G. Drubin. 1999. Novel protein kinases Ark1p and Prk1p associate with and regulate the cortical actin cytoskeleton in budding yeast. *J. Cell Biol.* 144:1203–1218. <https://doi.org/10.1083/jcb.144.6.1203>

Duncan, M.C., M.J. Cope, B.L. Goode, B. Wendland, and D.G. Drubin. 2001. Yeast Eps15-like endocytic protein, Pan1p, activates the Arp2/3 complex. *Nat. Cell Biol.* 3:687–690. <https://doi.org/10.1038/35083087>

Evangelista, M., B.M. Klebl, A.H. Tong, B.A. Webb, T. Leeuw, E. Leberer, M. Whiteway, D.Y. Thomas, and C. Boone. 2000. A role for myosin-I in actin assembly through interactions with Vrp1p, Bee1p, and the Arp2/3 complex. *J. Cell Biol.* 148:353–362. <https://doi.org/10.1083/jcb.148.2.353>

Feliciano, D., and S.M. Di Pietro. 2012. SLAC, a complex between Sla1 and Las17, regulates actin polymerization during clathrin-mediated endocytosis. *Mol. Biol. Cell.* 23:4256–4272. <https://doi.org/10.1091/mbc.E11-12-1022>

Freeman, N.L., T. Lila, K.A. Mintzer, Z. Chen, A.J. Pahk, R. Ren, D.G. Drubin, and J. Field. 1996. A conserved proline-rich region of the *Saccharomyces cerevisiae* cyclase-associated protein binds SH3 domains and modulates cytoskeletal localization. *Mol. Cell Biol.* 16:548–556. <https://doi.org/10.1128/MCB.16.2.548>

Goode, B.L., J.A. Eskin, and B. Wendland. 2015. Actin and endocytosis in budding yeast. *Genetics.* 199:315–358. <https://doi.org/10.1534/genetics.112.145540>

Goode, B.L., A.A. Rodal, G. Barnes, and D.G. Drubin. 2001. Activation of the Arp2/3 complex by the actin filament binding protein Abp1p. *J. Cell Biol.* 153:627–634. <https://doi.org/10.1083/jcb.153.3.627>

Huang, K.M., K. D'Hondt, H. Riezman, and S.K. Lemmon. 1999. Clathrin functions in the absence of heterotetrameric adaptors and AP180-related proteins in yeast. *EMBO J.* 18:3897–3908. <https://doi.org/10.1093/emboj/18.14.3897>

Huckaba, T.M., A.C. Gay, L.F. Pantalena, H.C. Yang, and L.A. Pon. 2004. Live cell imaging of the assembly, disassembly, and actin cable-dependent movement of endosomes and actin patches in the budding yeast, *Saccharomyces cerevisiae*. *J. Cell Biol.* 167:519–530. <https://doi.org/10.1083/jcb.200404173>

Kaksonen, M., and A. Roux. 2018. Mechanisms of clathrin-mediated endocytosis. *Nat. Rev. Mol. Cell Biol.* 19:313–326. <https://doi.org/10.1038/nrm.2017.132>

Kaksonen, M., Y. Sun, and D.G. Drubin. 2003. A pathway for association of receptors, adaptors, and actin during endocytic internalization. *Cell.* 115:475–487. [https://doi.org/10.1016/s0092-8674\(03\)00883-3](https://doi.org/10.1016/s0092-8674(03)00883-3)

Kaksonen, M., C.P. Toret, and D.G. Drubin. 2005. A modular design for the clathrin- and actin-mediated endocytosis machinery. *Cell.* 123:305–320. <https://doi.org/10.1016/j.cell.2005.09.024>

Kawada, D., H. Kobayashi, T. Tomita, E. Nakata, M. Nagano, D.E. Siekhaus, J.Y. Toshima, and J. Toshima. 2015. The yeast Arf-GAP Glo3p is required for the endocytic recycling of cell surface proteins. *Biochim. Biophys. Acta.* 1853:144–156. <https://doi.org/10.1016/j.bbamcr.2014.10.009>

Legendre-Guillemin, V., S. Wasiak, N.K. Hussain, A. Angers, and P.S. McPherson. 2004. ENTH/ANTH proteins and clathrin-mediated membrane budding. *J. Cell Sci.* 117:9–18. <https://doi.org/10.1242/jcs.00928>

Lila, T., and D.G. Drubin. 1997. Evidence for physical and functional interactions among two *Saccharomyces cerevisiae* SH3 domain proteins, an adenyl cyclase-associated protein and the actin cytoskeleton. *Mol. Biol. Cell.* 8:367–385. <https://doi.org/10.1091/mbc.8.2.367>

Lu, R., D.G. Drubin, and Y. Sun. 2016. Clathrin-mediated endocytosis in budding yeast at a glance. *J. Cell Sci.* 129:1531–1536. <https://doi.org/10.1242/jcs.182303>

Merrifield, C.J., M.E. Feldman, L. Wan, and W. Almers. 2002. Imaging actin and dynamin recruitment during invagination of single clathrin-coated pits. *Nat. Cell Biol.* 4:691–698. <https://doi.org/10.1038/ncb837>

Nolen, B., N. Tomašević, A. Russell, D. Pierce, Z. Jia, C.D. McCormick, J. Hartman, R. Sakowicz, and T. Pollard. 2009. Characterization of two classes of small molecule inhibitors of Arp2/3 complex. *Nature.* 460:1031–1034. <https://doi.org/10.1038/nature08231>

Rodal, A.A., A.L. Manning, B.L. Goode, and D.G. Drubin. 2003. Negative regulation of yeast WASp by two SH3 domain-containing proteins. *Curr. Biol.* 13:1000–1008. [https://doi.org/10.1016/s0960-9822\(03\)00383-x](https://doi.org/10.1016/s0960-9822(03)00383-x)

Smythe, E., and K.R. Ayscough. 2003. The Ark1/Prk1 family of protein kinases. Regulators of endocytosis and the actin skeleton. *EMBO Rep.* 4:246–251. <https://doi.org/10.1038/sj.embor.embor776>

Stefan, C.J., S.M. Padilla, A. Audhya, and S.D. Emr. 2005. The phosphoinositide phosphatase Sjl2 is recruited to cortical actin patches in the

- control of vesicle formation and fission during endocytosis. *Mol. Cell Biol.* 25:2910–2923. <https://doi.org/10.1128/MCB.25.8.2910-2923.2005>
- Sun, Y., N.T. Leong, T. Jiang, A. Tangara, X. Darzacq, and D.G. Drubin. 2017. Switch-like Arp2/3 activation upon WASP and WIP recruitment to an apparent threshold level by multivalent linker proteins in vivo. *Elife*. 6: e29140. <https://doi.org/10.7554/eLife.29140>
- Sun, Y., N.T. Leong, T. Wong, and D.G. Drubin. 2015a. A Pan1/End3/Slal complex links Arp2/3-mediated actin assembly to sites of clathrin-mediated endocytosis. *Mol. Biol. Cell.* 26:3841–3856. <https://doi.org/10.1091/mbc.E15-04-0252>
- Sun, Y., A.C. Martin, and D.G. Drubin. 2006. Endocytic internalization in budding yeast requires coordinated actin nucleation and myosin motor activity. *Dev. Cell.* 11:33–46. <https://doi.org/10.1016/j.devcel.2006.05.008>
- Sun, Y., N.T. Leong, T. Wong, and D.G. Drubin. 2015b. A Pan1/End3/Slal complex links Arp2/3-mediated actin assembly to sites of clathrin-mediated endocytosis. *Mol. Biol. Cell.* 26:3841–3856. <https://doi.org/10.1091/mbc.E15-04-0252>
- Suzuki, R., J.Y. Toshima, and J. Toshima. 2012. Regulation of clathrin coat assembly by Eps15 homology domain-mediated interactions during endocytosis. *Mol. Biol. Cell.* 23:687–700. <https://doi.org/10.1091/mbc.E11-04-0380>
- Tang, H.Y., J. Xu, and M. Cai. 2000. Pan1p, End3p, and Sla1p, three yeast proteins required for normal cortical actin cytoskeleton organization, associate with each other and play essential roles in cell wall morphogenesis. *Mol. Cell Biol.* 20:12–25. <https://doi.org/10.1128/MCB.20.1.12-25.2000>
- Toret, C.P., L. Lee, M. Sekiya-Kawasaki, and D.G. Drubin. 2008. Multiple pathways regulate endocytic coat disassembly in *Saccharomyces cerevisiae* for optimal downstream trafficking. *Traffic*. 9:848–859. <https://doi.org/10.1111/j.1600-0854.2008.00726.x>
- Toshima, J., J.Y. Toshima, M.C. Duncan, M.J.T.V. Cope, Y. Sun, A.C. Martin, S. Anderson, J.R. Yates 3rd, K. Mizuno, and D.G. Drubin. 2007. Negative regulation of yeast Eps15-like Arp2/3 complex activator, Pan1p, by the Hip1R-related protein, Sla2p, during endocytosis. *Mol. Biol. Cell.* 18: 658–668. <https://doi.org/10.1091/mbc.e06-09-0788>
- Toshima, J., J.Y. Toshima, A.C. Martin, and D.G. Drubin. 2005. Phosphoregulation of Arp2/3-dependent actin assembly during receptor-mediated endocytosis. *Nat. Cell Biol.* 7:246–254. <https://doi.org/10.1038/ncb1229>
- Toshima, J.Y., E. Furuya, M. Nagano, C. Kanno, Y. Sakamoto, M. Ebihara, D.E. Siekhaus, and J. Toshima. 2016. Yeast Eps15-like endocytic protein Pan1p regulates the interaction between endocytic vesicles, endosomes and the actin cytoskeleton. *Elife*. 5:e10276. <https://doi.org/10.7554/eLife.10276>
- Toshima, J.Y., J. Toshima, M. Kaksonen, A.C. Martin, D.S. King, and D.G. Drubin. 2006. Spatial dynamics of receptor-mediated endocytic trafficking in budding yeast revealed by using fluorescent alpha-factor derivatives. *Proc. Natl. Acad. Sci. USA.* 103:5793–5798. <https://doi.org/10.1073/pnas.0601042103>
- Watson, H.A., M.J. Cope, A.C. Groen, D.G. Drubin, and B. Wendland. 2001. In vivo role for actin-regulating kinases in endocytosis and yeast epsin phosphorylation. *Mol. Biol. Cell.* 12:3668–3679. <https://doi.org/10.1091/mbc.12.11.3668>
- Weinberg, J., and D.G. Drubin. 2012. Clathrin-mediated endocytosis in budding yeast. *Rev. Recent Clin. Trials.* 7:1–13. <https://doi.org/10.2174/157488712799363244>
- Wendland, B., and S.D. Emr. 1998. Pan1p, yeast eps15, functions as a multivalent adaptor that coordinates protein-protein interactions essential for endocytosis. *J. Cell Biol.* 141:71–84. <https://doi.org/10.1083/jcb.141.1.71>
- Wendland, B., K.E. Steece, and S.D. Emr. 1999. Yeast epsins contain an essential N-terminal ENTH domain, bind clathrin and are required for endocytosis. *EMBO J.* 18:4383–4393. <https://doi.org/10.1093/emboj/18.16.4383>
- Winter, D., T. Lechler, and R. Li. 1999. Activation of the yeast Arp2/3 complex by Bee1p, a WASP-family protein. *Curr. Biol.* 9:501–504. [https://doi.org/10.1016/s0960-9822\(99\)80218-8](https://doi.org/10.1016/s0960-9822(99)80218-8)
- Yamada, T., M.K. Owada, Y. Kitajima, and H. Kawakatsu. 1998. A rapid activation of Src tyrosine kinase and its binding to microtubules and nuclear envelope in cells at cut edges as a cultured wound model. *J. Invest Dermatol.* 110:497
- Zeng, G., X. Yu, and M. Cai. 2001. Regulation of yeast actin cytoskeleton-regulatory complex Pan1p/Sla1p/End3p by serine/threonine kinase Prk1p. *Mol. Biology Cell.* 12:3759–3772. <https://doi.org/10.1091/mbc.12.12.3759>

Supplemental material

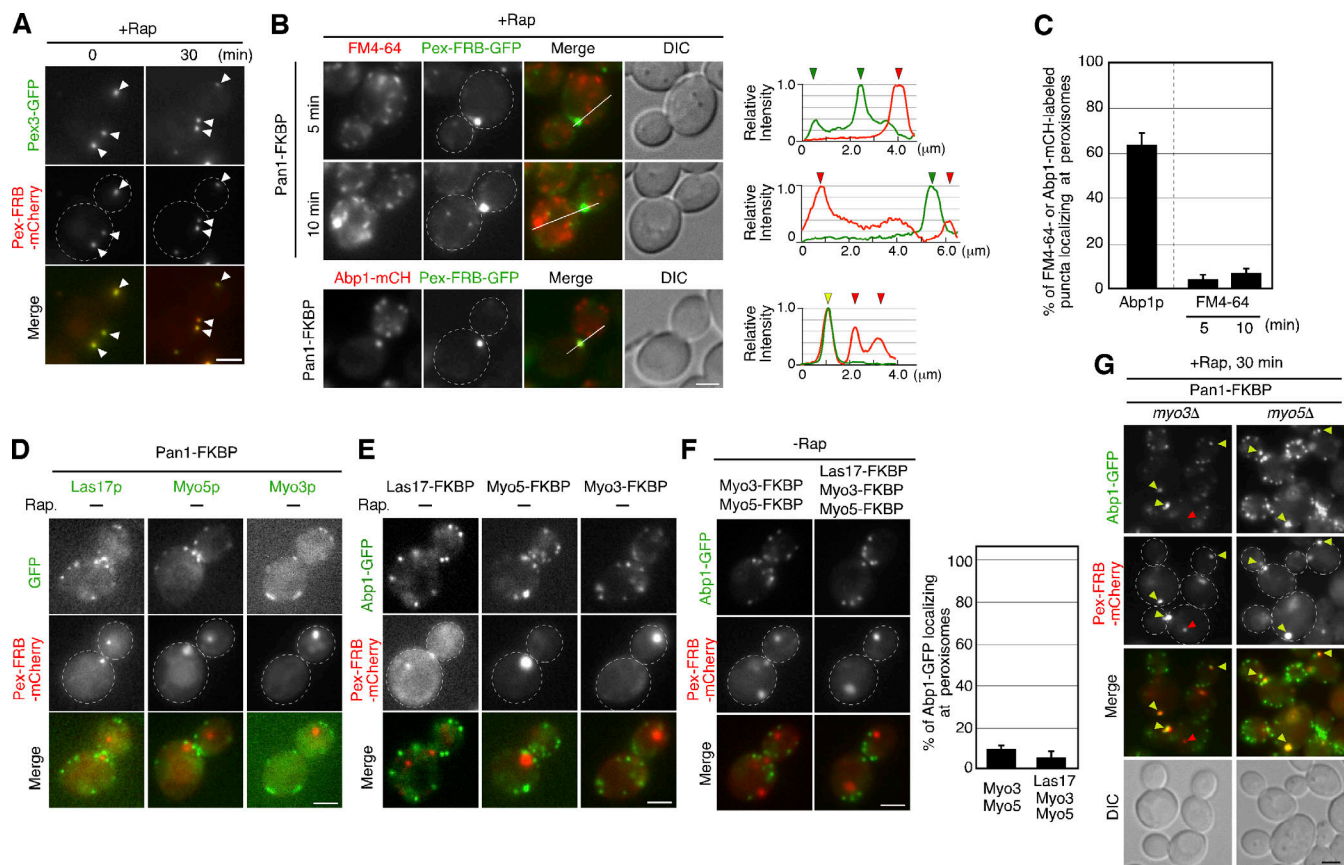


Figure S1. Targeting of Pan1p to the peroxisome leads to actin polymerization by recruiting other NPFs. (A) Localization of Pex3-GFP and Pex-FRB-mCherry at 0 or 30 min after rapamycin addition. White arrowheads indicate examples of co-localization. **(B)** Fluid-phase endocytosis in cells expressing Pan1-FKBP. Cells were labeled with 200 μM FM4-64 for 15 min on ice. The images were acquired at 5 or 10 min after FM4-64 internalization in the presence of rapamycin. The lower images show the localization of Abp1-mCherry and Pex-FRB-GFP at 30 min after rapamycin addition. Representative fluorescence intensity profiles along a line are indicated in the right panels. **(C)** The bar graph represents the percentages of FM4-64- or Abp1-mCherry-labeled puncta localizing at Pex-FRB-mCherry-labeled peroxisomes. Data show the mean from at least three experiments, with >50 cells counted for each strain per experiment. **(D)** Cells expressing GFP-tagged NPF (Las17p, Myo5p, or Myo3p), Pex-FRB-mCherry, and Pan1-FKBP were grown to log phase at 25°C, and each image pair was acquired before rapamycin addition. **(E)** Cells expressing Abp1-GFP, Pex-FRB-mCherry, and FKBP-tagged NPF were grown and imaged, as described in A. **(F)** The localization of Pex-FRB-mCherry and Abp1-GFP in cells expressing Las17-FKBP and/or Myo3/5-FKBP in the absence of rapamycin. Quantification of the percentage of Abp1-GFP co-localizing with Pex-FRB-mCherry-labeled peroxisomes is shown in the lower right panels. Data show the mean ± SD from three experiments ($n = 50$ puncta for each experiment). **(G)** The localization of Pex-FRB-mCherry and Abp1-GFP in *myo3Δ* or *myo5Δ* cells expressing Pan1-FKBP at 30 min after rapamycin addition. Scale bars, 2.5 μm.

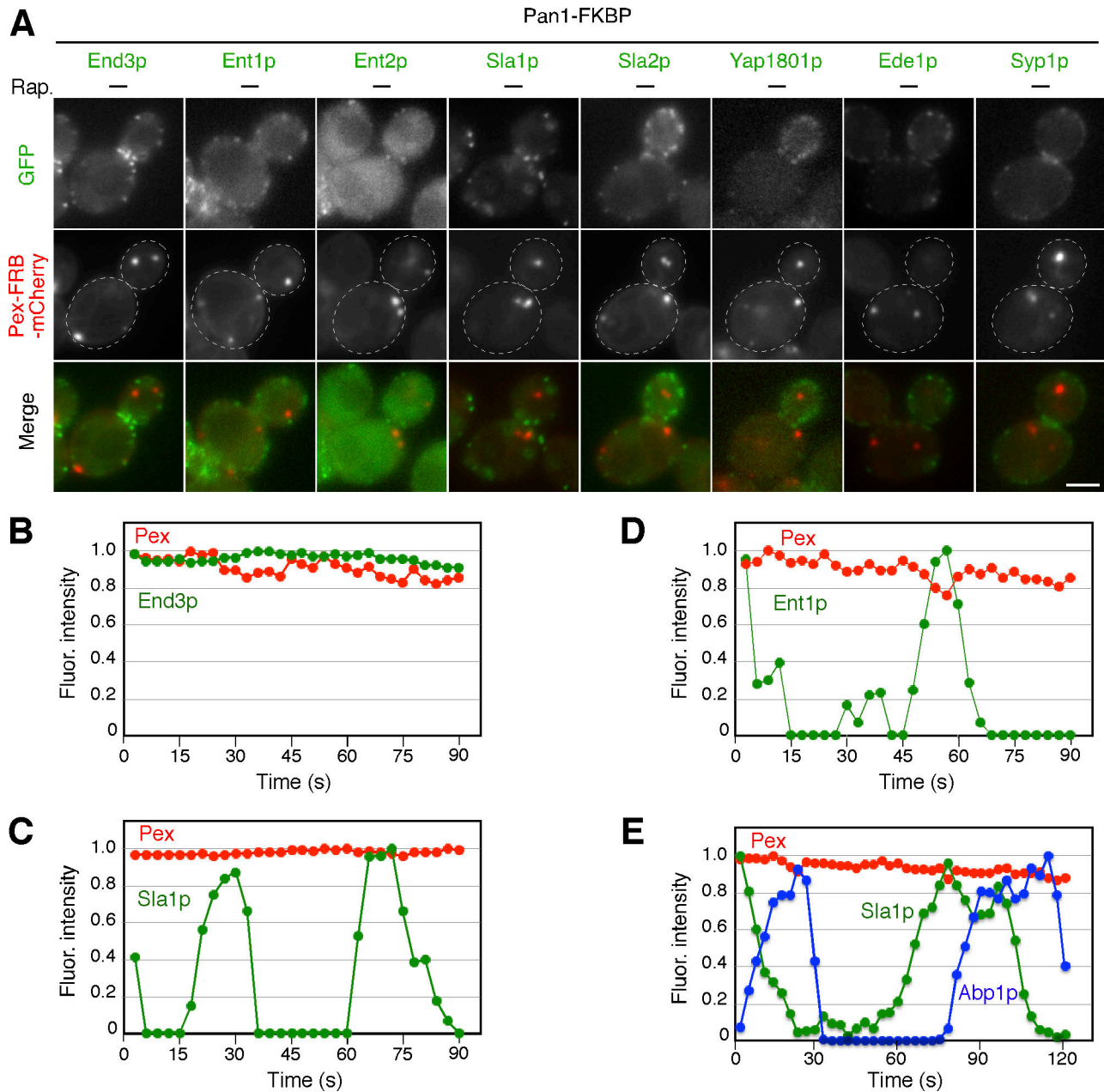


Figure S2. **Localization and fluorescence intensity of endocytic proteins at Pan1p-anchoring peroxisomes.** (A) Cells expressing GFP-tagged endocytic protein, Pex-FRB-mCherry, and Pan1-FKBP were grown to log phase at 25°C, and imaged before rapamycin addition. The upper and middle images show the individual channels and the low images shows the merged overlay of the signal from both channels. (B–D) Quantification of the normalized fluorescence intensities for indicated proteins in the boxed area of Fig. 6 (A, C, and E). (E) Quantification of the normalized fluorescence intensities of Pex-FRB-mCherry, Sla1-GFP and Abp1-Turquoise2 in the boxed area of Fig. 6 G. Scale bars, 2.5 μ m.

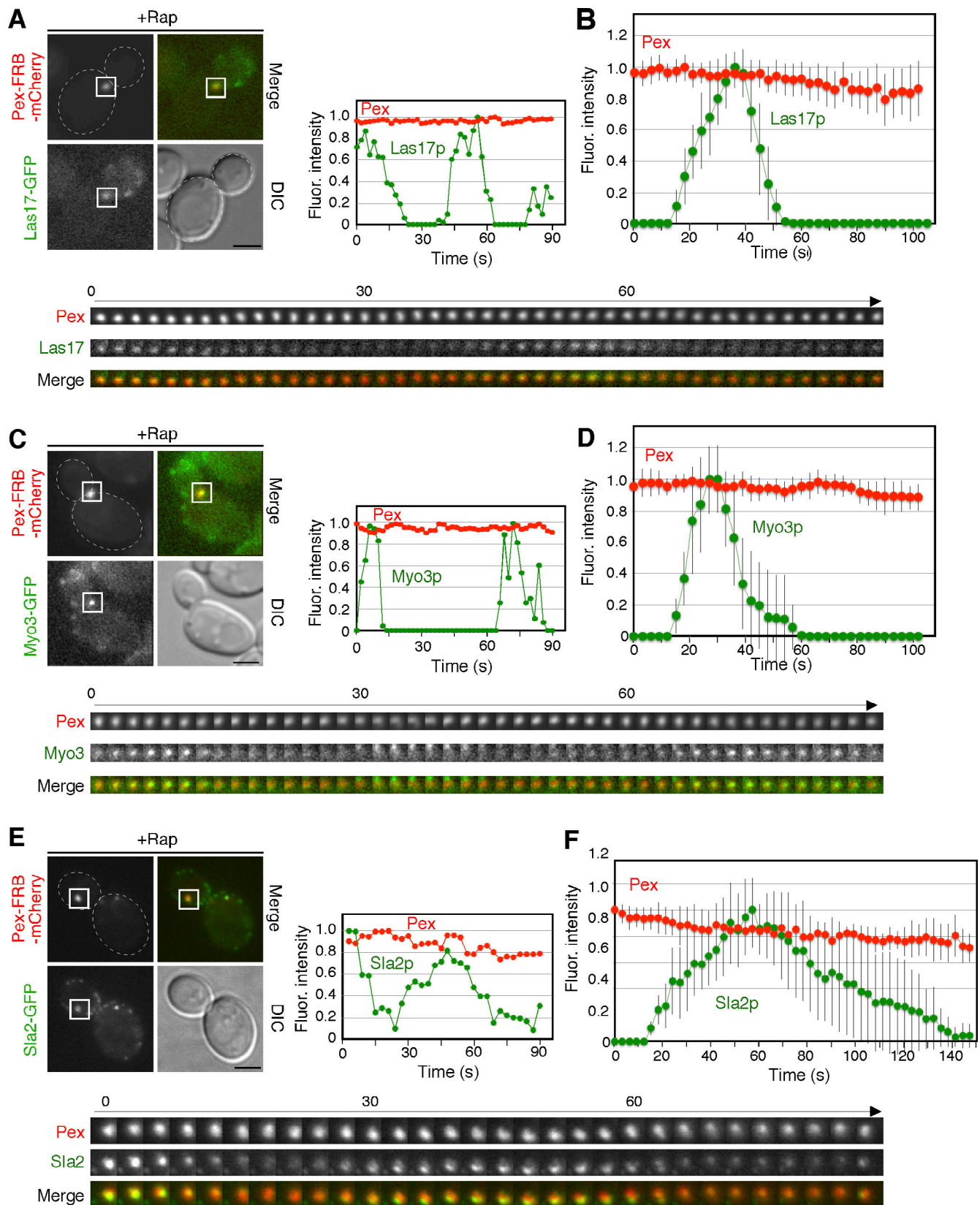


Figure S3. **Dynamic localization of endocytic proteins at Pan1p-anchoring peroxisomes. (A, C, and E)** The localization of Pex-FRB-mCherry and (A) GFP-fused Las17p, (C) Myo3p, or (E) Sla2p in cells expressing Pan1-FKBP at 30 min after rapamycin addition. The upper panels show single frames from movies of the indicated strain. A time series in the boxed area is shown in the lower panels. Quantification of the normalized fluorescence intensities of Pex-FRB-mCherry and the indicated GFP-fused protein at the boxed area is shown in right. **(B, D, and F)** Averaged fluorescence intensities as a function of time for each protein ($n = 10$ independent peroxisomes). Scale bars, 2.5 μm .

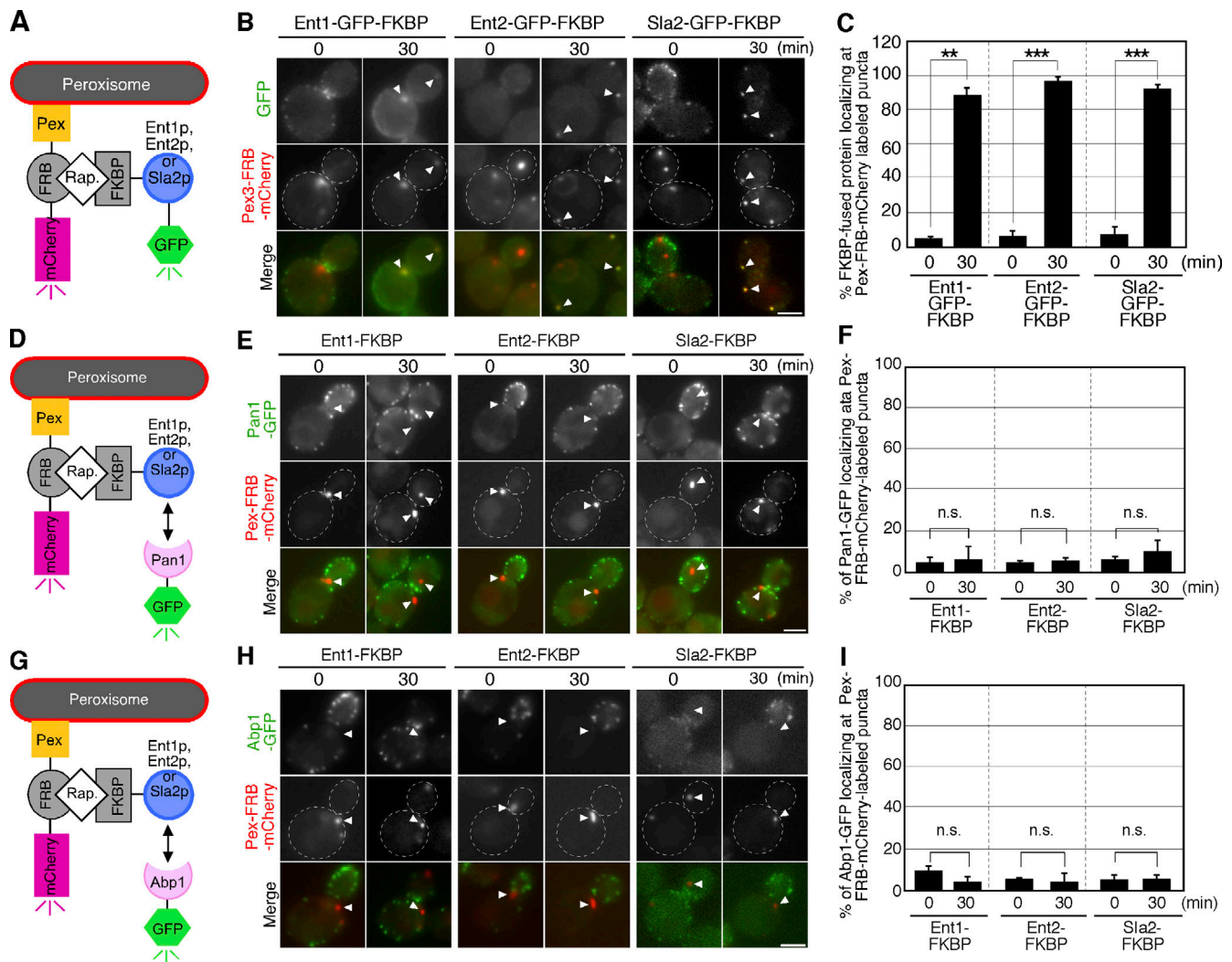


Figure S4. Ectopically localized Ent1p, Ent2p, and Sla2p cannot recruit Pan1p. (A) Schematic diagram of the inducible peroxisome redistribution assay. Ent1p, Ent2p, or Sla2p tagged with GFP and FKBP was co-expressed with the peroxisome-targeted Pex-FRB-mCherry fusion protein. Addition of rapamycin causes heterodimerization of FRB and FKBP and thereby recruits Ent1p, Ent2p, or Sla2p to the peroxisome surface. (B) Cells expressing Ent1-, Ent2, or Sla2-GFP-FKBP and Pex-FRB-mCherry were grown to log phase in YPD medium at 25°C, and each image pair was acquired before or at 30 min after rapamycin addition. White arrowheads indicate examples of co-localization. (C) Quantification of the percentages of the indicated GFP-FKBP tagged proteins co-localizing with Pex-FRB-mCherry-labeled peroxisomes before and after rapamycin addition. Data show the mean \pm SD from three experiments ($n = 50$ puncta for each experiment). (D and G) Schematic diagrams of the inducible peroxisome redistribution assay. Ent1p, Ent2p, or Sla2p tagged with FKBP was co-expressed with Pex-FRB-mCherry in cells expressing (D) GFP-tagged Pan1p or (G) Abp1p. (E and H) Localization of Pex-FRB-mCherry and Pan1-GFP (E) or Abp1-GFP (H) in the presence or absence of rapamycin. Cells were grown to log phase at 25°C and each image pair was acquired before or at 30 min after rapamycin addition. White arrowheads indicate localization of Pex-FRB-mCherry-labeled peroxisome. (F and I) Quantification of the percentages of Pan1-GFP (F) or Abp1-GFP (I) co-localizing with Pex-FRB-mCherry labeled peroxisomes before and after rapamycin addition. Data show the mean \pm SD from at least three experiments ($n \geq 50$ puncta for each experiment). ***, P value < 0.001, **, P value < 0.01, ns, non-statistically significant, unpaired *t* test with Welch's correction. Scale bars, 2.5 μ m.

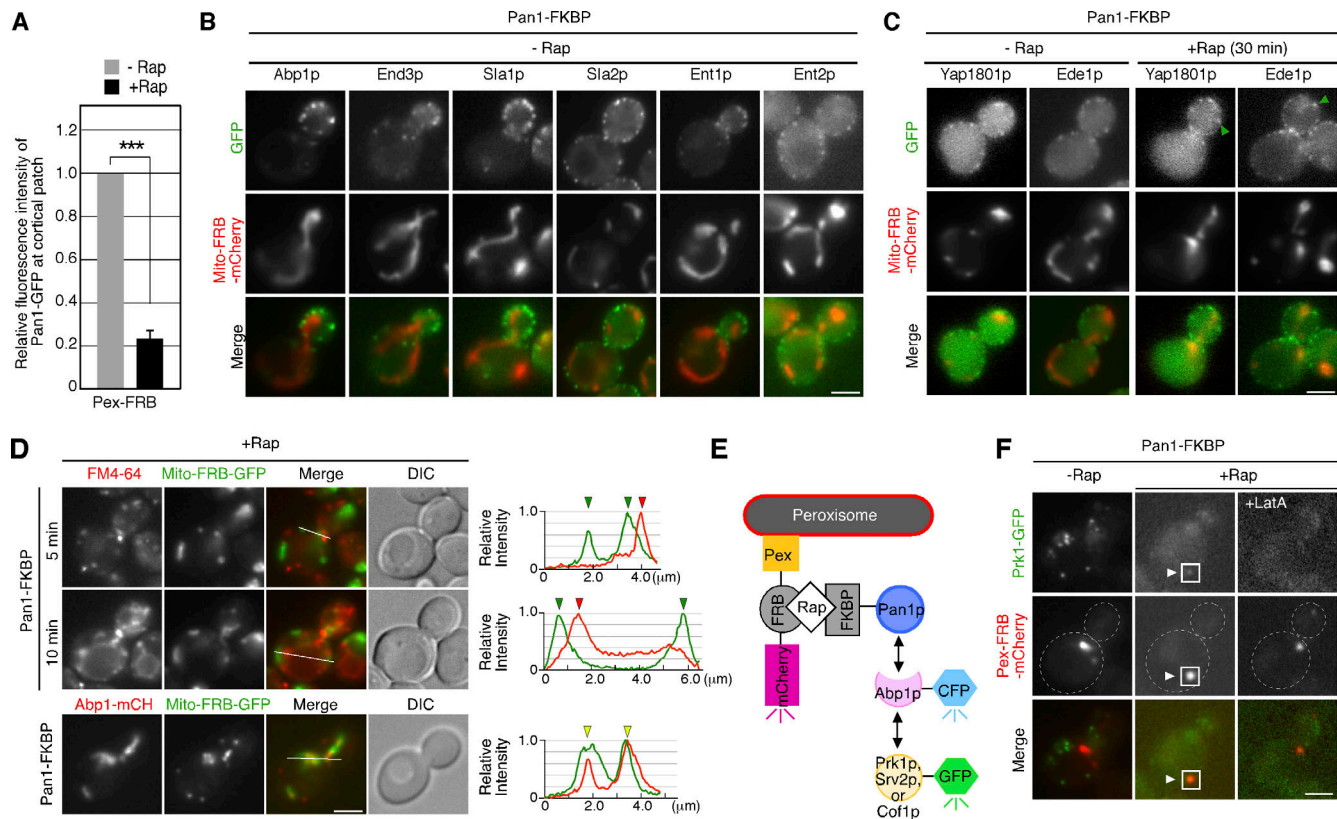


Figure S5. Localization of endocytic proteins in cells expressing Pan1-FKBP and Mito-FRB-mCherry, and Actin-dependent recruitment of Prk1-GFP to the Pan1p-anchoring peroxisome. (A) Relative localization of Pan1p at cortical patches in cells anchoring Pan1p to the peroxisome. Data show the mean \pm SD from three experiments ($n = 30$ patches for each experiment). ***, P value < 0.001 , unpaired t test with Welch's correction. (B) Localization of GFP-tagged endocytic proteins and Mito-FRB-mCherry before rapamycin addition. (C) Localization of GFP-tagged Yap1801p or Ede1p and Mito-FRB-mCherry before and at 30 min after rapamycin addition. (D) Fluid-phase endocytosis in cells expressing Mito-GFP-FRB and Pan1-FKBP. Cells were labeled with 200 μ M FM4-64 for 15 min on ice. The images were acquired at 5 and 10 min after FM4-64 internalization. Representative fluorescence intensity profiles along a line are indicated in the right panels. (E) Schematic diagram of the inducible peroxisome redistribution assay. Pan1-FKBP was co-expressed with Pex-FRB-mCherry in cells expressing GFP-tagged Prk1p, Srv2p, or Cof1p. Addition of rapamycin causes heterodimerization of FRB and FKBP and thereby recruits Pan1p and its binding protein to the peroxisome surface. (F) Localization of Prk1-GFP and Pex-FRB-mCherry before or 30 min after rapamycin addition. Cells were grown to log phase at 25°C. White arrowheads indicate examples of co-localization. Right image pair was acquired 30 min after rapamycin addition in the presence of 250 μ M LatA. Scale bar, 2.5 μ m.

Video 1. Dynamics of Pex-FRB-mCherry (red in merge) and Abp1-GFP (green in merge) on the peroxisome after washing away LatA. Wild-type cell expressing Pan1-FKBP, Pex-FRB-mCherry and Abp1-GFP was grown to log phase at 25°C, treated with 200 μ M LatA for 20 min at 15 min after rapamycin addition. Images were acquired every 20 s for 20 min at 20 min after washing away LatA, using a 100 \times objective on an Olympus IX83 microscope equipped with Orca-AG cooled CCD camera. The frame rate is 8 fps.

Video 2. Dynamics of Pex-FRB-mCherry (red in merge) and Abp1-GFP (green in merge). Wild-type cell expressing Pan1-FKBP, Pex-FRB-mCherry and Abp1-GFP was grown to log phase at 25°C, treated with 100 μ M CK-666 for 1 min 45 s at 30 min after rapamycin addition. The medium is then replaced with YPD containing rapamycin. Images were acquired every 5 s for 4 min, using a 100 \times objective on an Olympus IX83 microscope equipped with Orca-AG cooled CCD camera. The frame rate is 6 fps.

Video 3. Dynamics of Pex-FRB-mCherry (red in merge), Pan1-GFP-FKBP (green in merge), and Abp1-GFP (light blue in merge). Wild-type cell expressing Pex-FRB-mCherry, Pan1-GFP-FKBP, and Abp1-CFP was grown to log phase, treated with rapamycin for 30 min at 25°C. Images were acquired every 3 s for 1 min 30 s, using a 100 \times objective on an Olympus IX81 microscope equipped with Orca-AG cooled CCD camera. The frame rate is 8 fps.

Video 4. **Dynamics of Pex-FRB-mCherry (red in merge) and End3-GFP (green in merge).** Wild-type cell expressing Pan1-FKBP, Pex-FRB-mCherry and End3-GFP was grown to log phase, and treated with rapamycin for 30 min at 25°C. Images were acquired every 1.5 s for 1 min 30 s, using a 100× objective on an Olympus IX83 microscope equipped with Orca-AG cooled CCD camera. The frame rate is 8 fps.

Video 5. **Dynamics of Pex-FRB-mCherry (red in merge) and Sla1-GFP (green in merge).** Wild-type cell expressing Pan1-FKBP, Pex-FRB-mCherry and Sla1-GFP was grown to log phase, and treated with rapamycin for 30 min at 25°C. Images were acquired every 1.5 s for 1 min 30 s, using a 100× objective on an Olympus IX83 microscope equipped with Orca-AG cooled CCD camera. The frame rate is 8 fps.

Video 6. **Dynamics of Pex-FRB-mCherry (red in merge) and Ent1-GFP (green in merge).** Wild-type cell expressing Pan1-FKBP, Pex-FRB-mCherry and Ent1-GFP was grown to log phase, and treated with rapamycin for 30 min at 25°C. Images were acquired every 1.5 s for 1 min 30 s, using a 100× objective on an Olympus IX83 microscope equipped with Orca-AG cooled CCD camera. The frame rate is 8 fps.

Video 7. **Dynamics of Pex-FRB-mCherry (red in merge), Sla1-GFP (green in merge), and Abp1-mTq2 (light blue in merge).** Wild-type cell expressing Pan1-FKBP, Pex-FRB-mCherry, Sla1-GFP, and Abp1-CFP was grown to log phase, treated with rapamycin for 30 min at 25°C. Images were acquired every 3 s for 1 min 30 s, using a 100× objective on an Olympus IX81 microscope equipped with Orca-AG cooled CCD camera. The frame rate is 8 fps.

Video 8. **Dynamics of Pex-FRB-mCherry (red in merge), Prk1-GFP (green in merge), and Abp1-mTq2 (light blue in merge).** Wild-type cell expressing Pan1-FKBP, Pex-FRB-mCherry, Prk1-GFP, and Abp1-mTq2 was grown to log phase, treated with rapamycin for 30 min at 25°C. Images were acquired every 3 s for 1 min, using a 100× objective on an Olympus IX81 microscope equipped with Orca-AG cooled CCD camera. The frame rate is 8 fps.

Video 9. **Dynamics of Pex-FRB-mCherry (red in merge), GFP-Cof1 (green in merge), and Abp1-mTq2 (light blue in merge).** Wild-type cell expressing Pan1-FKBP, Pex-FRB-mCherry, GFP-Cof1, and Abp1-mTq2 was grown to log phase, treated with rapamycin for 30 min at 25°C. Images were acquired every 3 s for 1 min 27 s, using a 100× objective on an Olympus IX81 microscope equipped with Orca-AG cooled CCD camera. The frame rate is 8 fps.

Video 10. **Dynamics of Pex-FRB-mCherry (red in merge), Srv2-GFP (green in merge), and Abp1-mTq2 (light blue in merge).** Wild-type cell expressing Pan1-FKBP, Pex-FRB-mCherry, Srv2-GFP, and Abp1-mTq2 was grown to log phase, treated with rapamycin for 30 min at 25°C. Images were acquired every 3 s for 1 min 27 s, using a 100× objective on an Olympus IX81 microscope equipped with Orca-AG cooled CCD camera. The frame rate is 8 fps.

Video 11. **Dynamics of Pex-FRB-mCherry (red in merge), Abp140-3GFP (green in merge) after (upper panels) or after (lower panels) rapamycin addition.** Wild-type cell expressing Pan1-FKBP, Pex-FRB-mCherry, and Abp140-3GFP was grown to log phase. Images were acquired every 1 s for 39 s in the presence (upper video) or absence (lower video) of rapamycin, using a 100× objective on an Olympus IX83 microscope equipped with Orca-AG cooled CCD camera. The frame rate is 8 fps.

Provided online are Table S1, Table S2, and Data S1. Table S1 shows yeast strains. Table S2 lists primer sequences for PCR. Data S1 contains data for LatA treatment and recovery in Fig. 1 F.